Lehrstuhl für Raumfahrttechnik

Prof. Prof. h.c. Dr. Dr. h.c.
Ulrich Walter

Technische Universität München

Semesterarbeit

Communication-concept with Relay Satellites for Excursions to the Lunar South Pole

RT-SA 2020/18

Autor:

B.Sc. Michael Huber

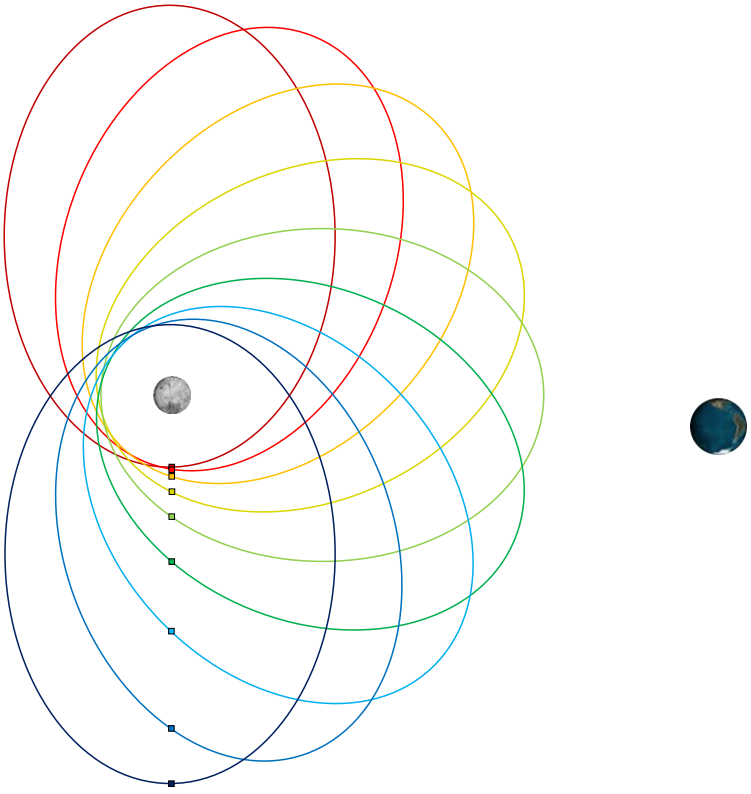

Betreuer: M.Sc. Daniel Kaschubek
Lehrstuhl für Raumfahrttechnik / Institute of Astronautics
Technische Universität München

Acknowledgments

This paper would not have been possible without the constant feedback and great support of all my advisors, and I would like to thank them all for their guidance.

Thank you to my advisors at the German Aerospace Center (DLR), Dr. Dieter Sabath and Gerd Söllner, for the great insights you gave me about the human presence in space and your constant feedback.

Thank you to my advisor at TUM, M.Sc. Daniel Kaschubek, for the constant support during the writing of this thesis.

Zusammenfassung

Derzeit sind mehrere Missionen zur Mondoberfläche in Planung. Dazu gehört auch das Artemis-Programm der NASA, welches bis 2024 wieder Menschen auf der Mondoberfläche landen soll. Eine unterbrechungsfreie Kommunikation ist ein wesentliches Sicherheitselement der Mission. In dieser Arbeit werden die möglichen Landegebiete und ihre Topographie analysiert, um anschließend eine detaillierte Simulation der Kommunikation zwischen der Erde und diesen Gebieten durchzuführen. Ziel ist es, das bestmögliche Kommunikationssystem für Exkursionen zum Mondsüdpol mit möglichst geringem Ressourceneinsatz zu finden und dabei auch alle anderen geplanten Missionen zu berücksichtigen.

Ein im Rahmen dieser Arbeit geschriebenes MATLAB®-Skript analysiert die Topographie an potenziell interessanten Regionen am Mondsüdpol anhand der von der NASA veröffentlichten DEM-Daten. Es ermittelt die genauen Landeplätze, die die beste Kommunikation ermöglichen. Die Analyse ergibt, dass nur wenige lokale Bergspitzen um das Malapert- und das Leibnitz-Massiv eine ununterbrochene direkte Kommunikation mit der Erde ermöglichen. Diese Orte wären daher die Hauptkandidaten für Landeplätze bei der ersten Rückkehr der Menschen zum Mond. Alle anderen potenziellen Landeplätze benötigen Relay-Satelliten in der Mondumlaufbahn, um eine durchgehende Abdeckung zu erreichen. Eine Simulation mehrerer Konstellationstypen ergibt, dass für eine vollständige Abdeckung des Südpols mindestens zwei Relay-Satelliten in der Mondumlaufbahn erforderlich sind. Der Plan der NASA für die Rückkehr zum Mond sieht die Installation des Lunar Gateway vor, einer Raumstation in einem Near-Rectilinear Halo Orbit (NRHO). Dies ist ein südlicher Halo Orbit im L2-Punkt mit in einer 9:2-Resonanz mit der synodischen Periode des Mondes. Die stark elliptische Umlaufbahn des Gateway mit einer Apoapsis über dem Mondsüdpol kann in 97% der Zeit eine Sichtlinie zum Mondsüdpol herstellen. Es ist fester Bestandteil des Artemis-Programms der NASA und ist in der Lage als Relay-Knoten zu fungieren.

Weitere interessante Orte für künftige Missionen auf der Mondoberfläche sind der Nordpol und die Rückseite des Mondes. Das Gateway allein erreicht eine durchschnittliche Abdeckung der Rückseite des Mondes von 54,50%, eine maximale Abdeckung der Rückseite von über 97,43% zwischen -80° und 80° geografischer Breite, aber nur eine Abdeckungszeit von 1,12% am Nordpol. Ein im Rahmen dieser Arbeit geschriebenes MATLAB®-Skript mit einer Schnittstelle zum System Tool Kit von AGI analysiert, wie das Gateway am besten in eine Relay-Satellitenkonstellation implementiert werden kann. Das Skript simuliert zusätzliche Satelliten um den Mond und misst die von der Konstellation erreichte Abdeckung in verschiedenen Regionen der Mondoberfläche. Ein Bewertungssystem evaluiert und bestimmt die beste Konstellation. Es berücksichtigt die Dauer der Kommunikationslücken, die Abdeckung mehrerer interessanter Regionen am Südpol, die Abdeckung von Regionen am Südpol mit höherer Topographie, die Abdeckung am Mondnordpol und die Abdeckung der Mondrückseite. Eine Konstellation, bestehend aus dem Gateway und einem Satelliten mit den folgenden Merkmalen, erreichte die höchste Gesamtpunktzahl: eine Apoapsis-Höhe von 54329,13059 km, eine Periapsis-Höhe von 10527 km, eine Inklination von 90°, ein Periapsis-Argument von 270° und eine wahre Anomalie, die so eingestellt ist, dass sie über dem Südpol liegt, wenn das Gateway seine Periapsis über dem Nordpol erreicht. Diese Konstellation erreicht eine Abdeckung von 100,00% für alle

potenziellen Landegebiete am Südpol und bietet außerdem eine Abdeckung von 87,71% am Nordpol, eine Abdeckung von 99,99% an einem Punkt auf der Rückseite des Mondes zwischen -80° und 80° geografischer Breite, eine durchschnittliche Abdeckung der Rückseite des Mondes von 89,30% und eine Abdeckung von 100,00% in der Mitte des Shackleton-Kraters.

Diese Ergebnisse zeigen, dass die für alle geplanten Missionen zur Mondoberfläche benötigte Kommunikation durch den Start eines einzigen zusätzlichen Satelliten in die Mondumlaufbahn erreicht werden kann.

Abstract

Currently, multiple missions to the lunar surface are being planned. This includes NASA's Artemis program which intends on landing humans back on the surface of the Moon by 2024. Uninterrupted communication is a key safety element of the mission. This paper analyzes the possible landing regions and their topography for a subsequent detailed simulation of the communication between the Earth and those regions. The objective is to find the best possible communication system for excursions to the lunar south pole using as little resources as possible while also considering all the other planned missions.

A MATLAB® script written within the scope of this paper analyzes the topography around potential regions of interest at the lunar south pole using DEM-data published by NASA. It determines the exact landing sites which allow for the best communication. This analysis unveiled that only few local mountain peaks around the Malapert and Leibnitz Massifs allow for uninterrupted direct communication to the Earth. These spots would therefore be prime candidates for landing sites when humans first return to the lunar surface. All other potential landing sites need relay satellites in lunar orbit to achieve full coverage. A simulation of multiple constellation types determined that at least two relay satellites in lunar orbit are necessary for full south pole coverage. NASA's plan to return to the Moon includes the installation of the Lunar Gateway, a space station in a Near-Rectilinear Halo Orbit (NRHO) which is a L2 southern halo orbit in a 9:2 resonance with the lunar synodic period. The Gateway's highly elliptical orbit with an apoapsis above the lunar south pole can establish a line of sight to the lunar south pole over 97% of the time. It is a fixed part of NASA's Artemis Program and will be capable of acting as a communication relay node.

Other places of interest for future missions on the lunar surface are the north pole and the far side. The Gateway alone achieves an average far side coverage time of 54.50%, a maximum far side coverage of over 97.43% between -80° and 80° latitude but only a 1.12% coverage time at the north pole. A MATLAB® script with an interface to AGI's System Tool Kit written within the scope of this paper analyzes how the Gateway can be best implemented into a relay satellite constellation. The script simulates additional satellites around the Moon and measures the coverage achieved by the constellation at different regions on the lunar surface. A scoring system evaluates and determines the best overall constellation. It considers the communication gap durations, the coverage at multiple regions of interest at the south pole, the coverage around regions at the south pole with higher topography, the coverage at the lunar north pole and the coverage at the lunar far side. A constellation consisting of the Gateway and a satellite with the following traits attained the overall highest score: an apoapsis height of 54329.13059 km, a periapsis height of 10527 km, an inclination of 90°, an argument of periapsis of 270° and a true anomaly set to be above the south pole as the Gateway reaches its periapsis above the north pole. This constellation achieves 100.00% coverage for all potential landing regions at the south pole while also providing 87.71% coverage at the north pole, 99.99% coverage on a point on the far side of the Moon between -80° an 80° latitude, 89.30% average far side coverage and 100.00% coverage in the middle of the Shackleton crater.

These results show that the communication needed for all the planned missions to the lunar surface can be achieved by launching just one additional satellite into lunar orbit.

Table of Contents

List of Figures

List of Tables

Symbols and Formulas

R_{moon}:	[m]	Mean Lunar Radius used in the DEM data
h_i:	[m]	Height above the Mean Lunar Radius
x_i:	[m]	Distance between two points
α_i:	[°]	Angle between two lines
β:	[°]	Central Angle between two points on the Lunar Surface
d:	[m]	Shortest Distance between two points
e:	[°]	Elevation Angle
θ_1:	[°]	Latitude Viewpoint
θ_2:	[°]	Latitude Observed Point
λ_1:	[°]	Longitude Viewpoint
λ_2:	[°]	Longitude Observed Point
s:	[-]	Score of the Constellation
t_{Gap}:	[s]	Maximum Gap Duration
$t_{GapAllowed}$:	[s]	Maximum Allowed Gap Duration
c_{Sha}:	[%]	Coverage inside the Shackleton Crater
c_{NP}:	[%]	North Pole Coverage
c_{AFS}:	[%]	Average Far Side Coverage
c_{MFS}:	[%]	Maximum Far Side Coverage
w_{Gap}:	[-]	Weighting of Gap Duration score
w_{Sha}:	[-]	Weighting of Shackleton Coverage score
w_{NP}:	[-]	Weighting of North Pole Coverage score
w_{AFS}:	[-]	Weighting of Average Far Side Coverage score
w_{MFS}:	[-]	Weighting of Maximum Far Side Coverage score

Abbreviations

Fig.	Figure	Tab.	Table
DLR	German Aerospace Center	LOFAR	Low Frequency Array
LRO	Lunar Reconnaissance Orbiter	LOLA	Lunar Orbiter Laser Altimeter
DEM	Digital Elevation Model	AzEl	Azimuth Elevation
STK	AGI's System Tool Kit	NRHO	Near-Rectilinear Halo Orbit

1 Introduction

1.1 Objectives of Lunar Exploration

Ever since the first humans stepped foot on the lunar surface from 1969 to 1972 as part of the Apollo program, none have returned thereafter. The footprints made by the twelve astronauts are still intact to this day as the Moon has no atmosphere or plate tectonics. A monument for eternity to one of humanity's greatest achievements. Up to this day, the Moon is still the only celestial body besides the Earth humans have ever visited. We can learn a great deal about ourselves and our own planet by studying our natural satellite.

The lack of erosion on the lunar surface makes it a witness to 4.5 billion years of solar system history. The Moon is the purest known record of geological processes of early planetary evolution. It shares insights of the early history of the Earth-Moon system, it can show the evolution of other terrestrial planets such as Mars and Venus and it can reveal the history of asteroid impacts in the inner solar system. But in order to study these processes, new samples from regions of the Moon that have never been visited before are necessary. [1, p. 1]

The Moon can not only be used to study our solar system. It also allows for superb interstellar observations through radio telescopes when they are placed on the far side of the Moon. A radio telescope placed there would be completely isolated from any interference of light with an atmosphere and any infrared and radio light emitted from the Sun and the Earth, which allows for high quality observation of faraway galaxies. [2]

Because of its closeness to the Earth, the Moon provides an ideal first testing ground for the technologies needed to reach even further destinations such as Mars. It could even be used as a hub station for a larger interplanetary infrastructure because of its low gravity and the occurrence of ice at the lunar poles, which can be used to produce drinkable water and rocket fuel.

1.2 The Lunar South Pole

In 2009, NASA reported that the Moon Mineralogy Mapper Spectrometer onboard India's ISRO Chandrayaan-1 probe has detected absorption features on the surface of the Moon, which are typically attributed to OH and H_2O bearing materials. Onboard Chandrayaan-1 was the Moon Impact Probe which was crashed into Shackleton crater at the lunar south pole and confirmed the presence of water ice. It is assumed that this is an ongoing surficial process where solar winds containing hydrogen are trapped at so called permanently shadowed regions. [3, p. 1]

Because the Sun's light hits the Moon's poles at a very low angle, there are regions in the middle of impact craters near the south pole where no sunlight has hit the surface for billions of years [4, p. 184]. The Sun's radiation would lead to the decomposition of the water ice and with no global magnetic field or atmosphere the solar winds would slowly carry the atoms away from the Moon and into space. But in these cold traps, the water ice remains uninterrupted [4, p. 192]. As the lunar south pole has more craters than the north pole and therefore more permanently shadowed regions, more

ice is detected there compared to the lunar north pole (Fig. 1-1). Another big advantage of the lunar poles is the existence of local mountain peaks reaching a solar illumination of up to 92.27% at 2 m above ground [5, p. 78]. This allows solar panels generate electricity most of the time, which makes the lunar poles the prime candidates for human habitation.

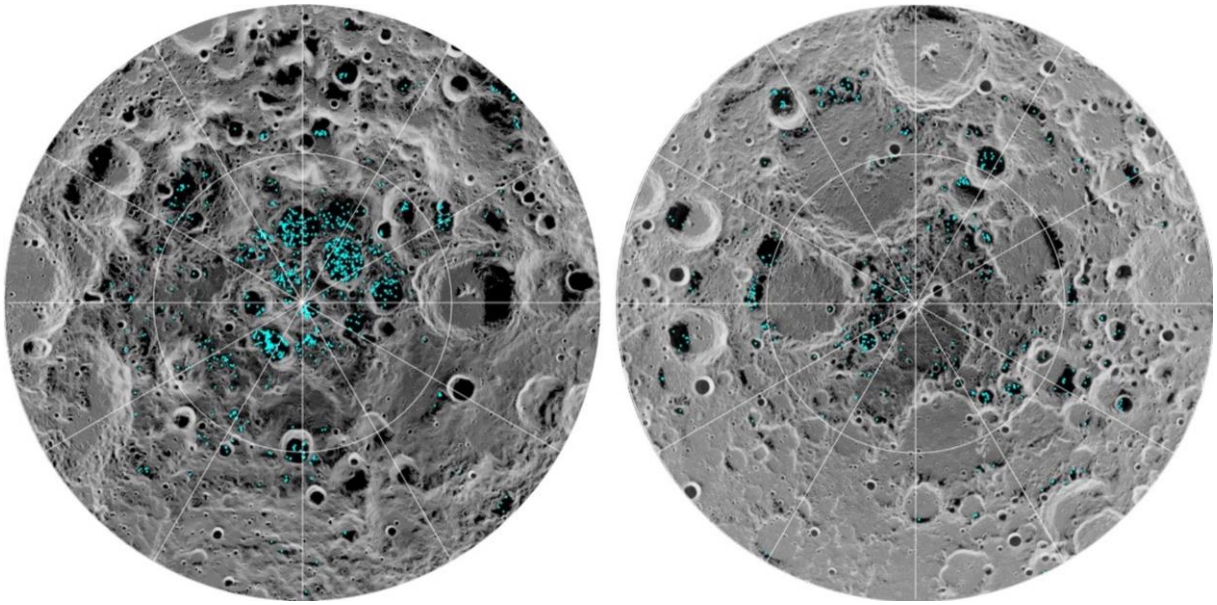

Fig. 1-1 Distribution of surface ice at the Moon's south pole (left) and north pole (right), detected by NASA's Moon Mineralogy Mapper instrument. Blue represents the ice locations. The ice is located in the darkest and coldest locations, the shadowed craters. The figure is taken from [6].

1.3 Currently Planned Missions

NASA is planning on landing humans back on the surface of the Moon by 2024 with the Artemis program. The uncrewed Artemis I maiden flight of the integrated Space Launch System rocket and the Orion spacecraft will verify the systems performance before launching humans on their way to the Moon with the Artemis II mission. This second flight of the system will be a 10-day crewed test flight which will orbit the Moon and will set a record for the farthest human travel from the Earth. In 2024, the Artemis III mission will launch humans to the lunar surface. Afterwards, NASA and its commercial and international partners have set the goal to build a permanent presence on the Moon with the Artemis Base Camp. [7]

The Lunar Orbital Platform – Gateway is an important part of NASA’s long-term plan of human space exploration. The Gateway will be a space station in cislunar space enabling a sustained presence around and on the Moon with lunar landers docking to the Gateway before descending to the lunar surface. The Gateway will also deploy critical infrastructure required for other deep space destinations such as Mars. The Gateway will be positioned on a Near-Rectilinear Halo Orbit (NRHO) around the L2-point of the Earth-Moon-System. [8], [9, pp. 1-2]

ESA is currently developing the LOFAR (Low Frequency Array), the next generation radio telescope, aimed to be placed on the far side of the Moon. It is expected that LOFAR could find about 100 million new sources of stars, planets, star forming

galaxies, active black holes and the first objects in the universe after the Big Bang. Instead of placing a small number of big antennas on the lunar surface, the LOFAR system will use many smaller and cheaper ones which still allows for an improvement in resolution and sensitivity by two orders of magnitude. [2]

1.4 Communication Requirements for Human Lunar South Pole Expeditions

Communication is a critical part of safety for all human spaceflight missions. Robotic missions allow for longer communication gaps during which a rover or a probe will simply wait for a new signal to emerge. Astronauts could experience emergency situations during a signal loss where feedback and instructions from the ground station could help saving the astronaut's life and the mission. Together with the help of employees from the German Aerospace Center (DLR, "Deutsches Zentrum für Luft- und Raumfahrt") it was determined that a maximum communication gap of ten minutes could be allowed for human missions to the lunar south pole, based on the experience gathered by the administration of the ISS[1]. This maximum value will be used for the further analysis in this paper.

1.5 Objectives of this Paper

The objective of this paper is to determine which satellite relay constellation is most suitable for the planned missions to the lunar surface. The focus lies on the communication coverage of the lunar south pole for a sustained presence and habitation there. The other aspects of lunar exploration, the north pole and the far side, will be used to better evaluate the different constellations. If two constellations provide a perfect south pole coverage, the one allowing for better north pole and far side coverage is determined as more suitable. This paper will also investigate the possibility of direct communication between the lunar surface and the Earth after determining the most suitable locations on the Moon through an analysis of the surrounding topography. Additionally, this paper analyzes the capabilities of the Lunar Gateway as a communication relay node and how it can be implemented into a satellite relay constellation.

[1] Personal communication with Dr. Dieter Sabath (Columbus MOS Manager) and Gerd Söllner (Columbus MOS Manager) part of the COL-CC Integrated Team at the German Aerospace Center (DLR) in Oberpfaffenhofen.

2 Potential Regions of Interest at the Lunar South Pole

2.1 Candidates Landing Sites Determined by NASA and TUM

While NASA has not yet determined the landing site for the Artemis III Mission, several interesting regions near permanently shadowed areas were chosen, which may contain mission-enhancing volatiles. These regions were selected as they may also offer long-duration access to sunlight, surface slope and roughness that will be less challenging for landers and astronauts (Fig. 2-1). [10, p. 7]

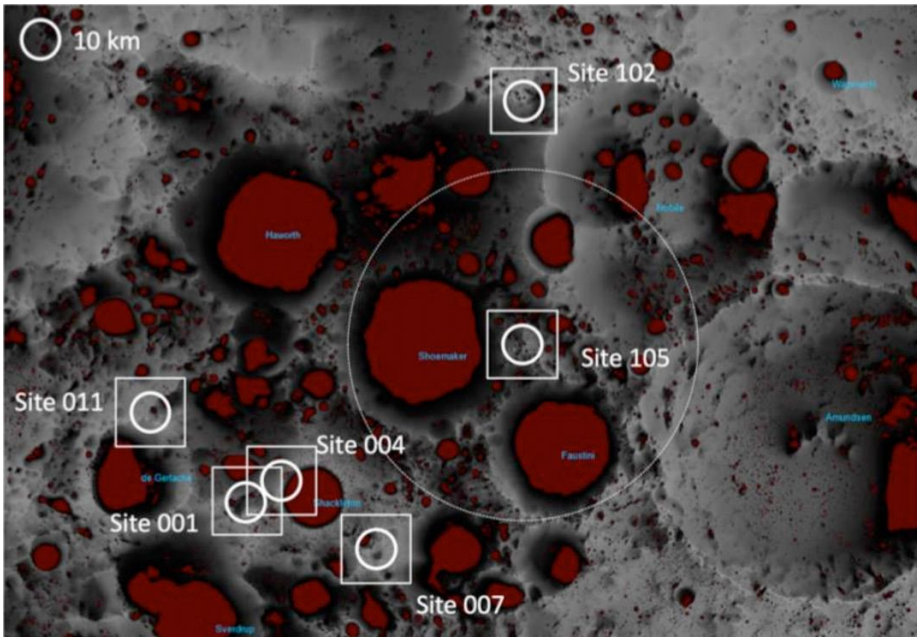

Fig. 2-1 The regions of interest determined in NASA's Plan for Sustained Lunar Exploration and Development. The figure is taken from [10, p. 9].

The encircled candidate regions have a diameter of 10 km. From Fig. 2-1 the centers' coordinates can be determined. A paper released by the Chair of Astronautics at the Technical University of Munich also determined another region fitting the given criteria [11]. It is located on a hill near the Kocher crater and was therefore called "Mount Kocher". For the following analysis it will also be viewed as a circular region with a diameter of 10 km. These seven regions shown in Tab. 2-1 and Fig. 2-2 will form the basis for the following analysis.

Tab. 2-1 Coordinates of the potential landing regions.

Landing Region	Latitude	Longitude
S001	-89.4949°	-119.0137°
S004	-89.9225°	-106.6992°
S007	-88.8460°	128.6023°
S011	-88.4262°	-64.5831°
S102	-85.4465°	32.0845°
S105	-87.2296°	-60.3789°
Mount Kocher	-85.6827°	-116.6140°

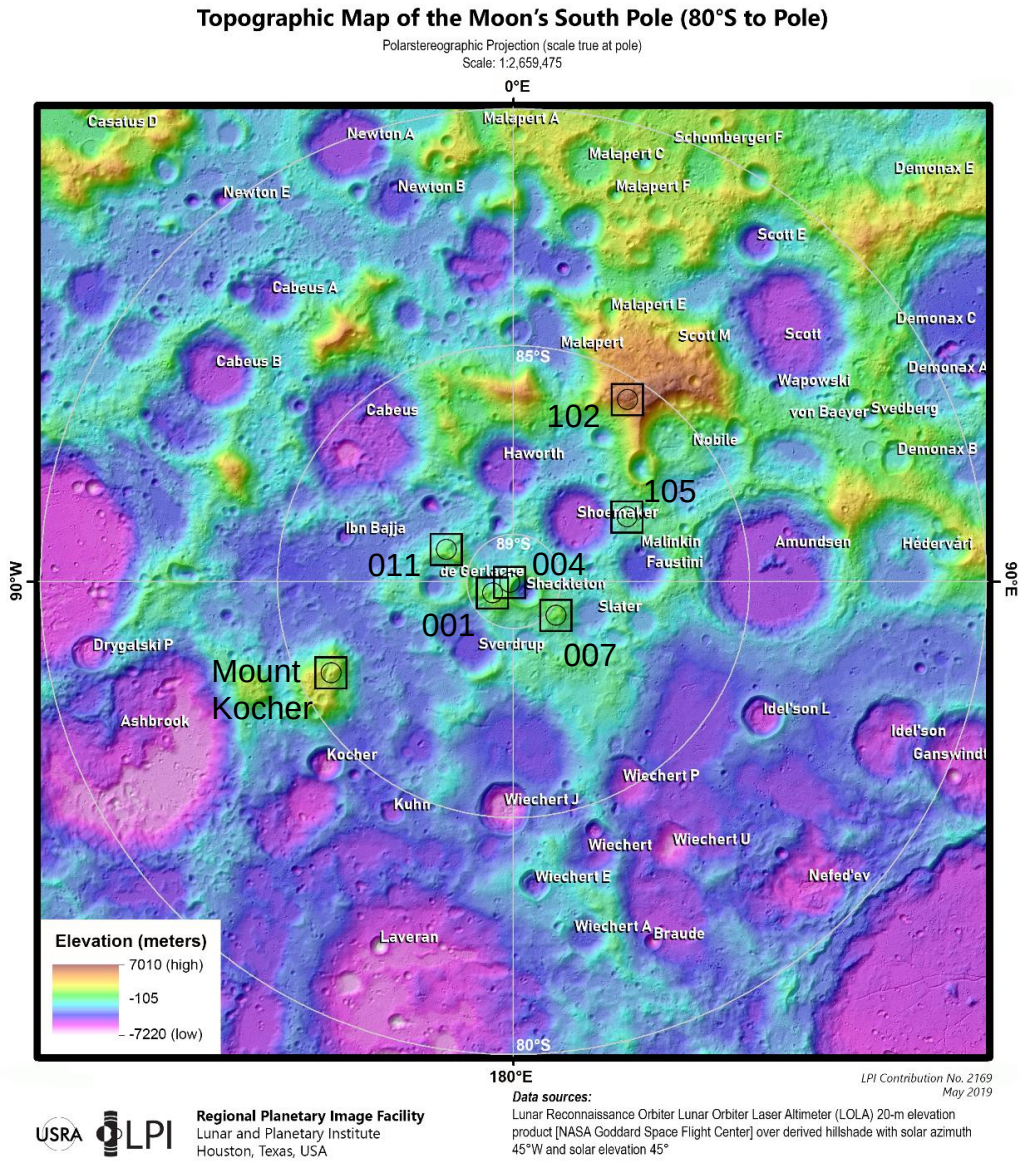

Fig. 2-2 The potential landing regions used for the following analysis. The black circles and quadrats are added to the Topographic Map of the Moon's South Pole taken from [12].

2.2 Optimal Locations for Communication on the Lunar Surface

2.2.1 Local Horizon Approach to Identify Optimal Locations

To further analyze the communication to the landing regions, a local horizon algorithm will find the best possible locations for communication within the 10 km circular landing regions from Tab. 2-1. As the Moon has no atmosphere, communication with satellites is possible at very low elevation angles. Therefore, the only restriction is the topology of the Moon itself as communicating with an overhead bypassing satellite is possible as soon as the satellite appears above the horizon. Thus, the best possible location for communication is the point with the lowest local horizon and therefore the lowest azimuth elevation mask (Fig. 2-3).

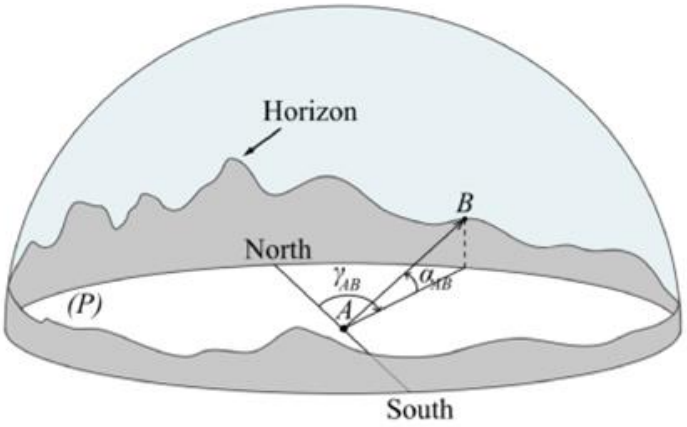

Fig. 2-3 Depiction of the azimuth and elevation angles as a result of the local horizon (α = elevation angle, γ = azimuth angle). The figure is taken from [13].

In 2008 NASA launched the Lunar Reconnaissance Orbiter (LRO) carrying the Lunar Orbiter Laser Altimeter (LOLA) which measured the global topography of the lunar surface at a high resolution. [14, pp. 391-392]

NASA published a Digital Elevation Model (DEM) of the lunar south pole with a resolution of 30 m/pix based on the LOLA data. The data set represents a stereographic projection of the surface which is true to scale at the south pole and is therefore the map projection best suited for analyses near the south pole. [15]

This data set provides the required topography for an analysis of the local horizon of the landing regions and determining the best location for communication. For this purpose, the MATLAB® script “Local_Horizon.m” was written within the scope of this paper. The script reads the data provided by NASA and calculates the azimuth elevation mask by calculating the elevation angle between the viewpoint and all surrounding pixels (Fig. 2-4 and Fig. 2-5).

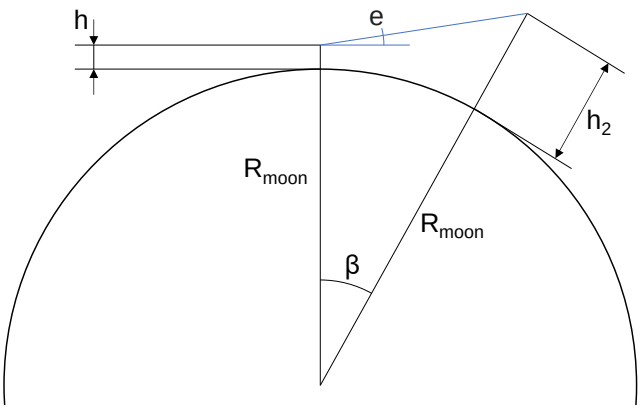

Fig. 2-4 Calculation of the elevation angle e with the height data h and h_2 from the DEM data.

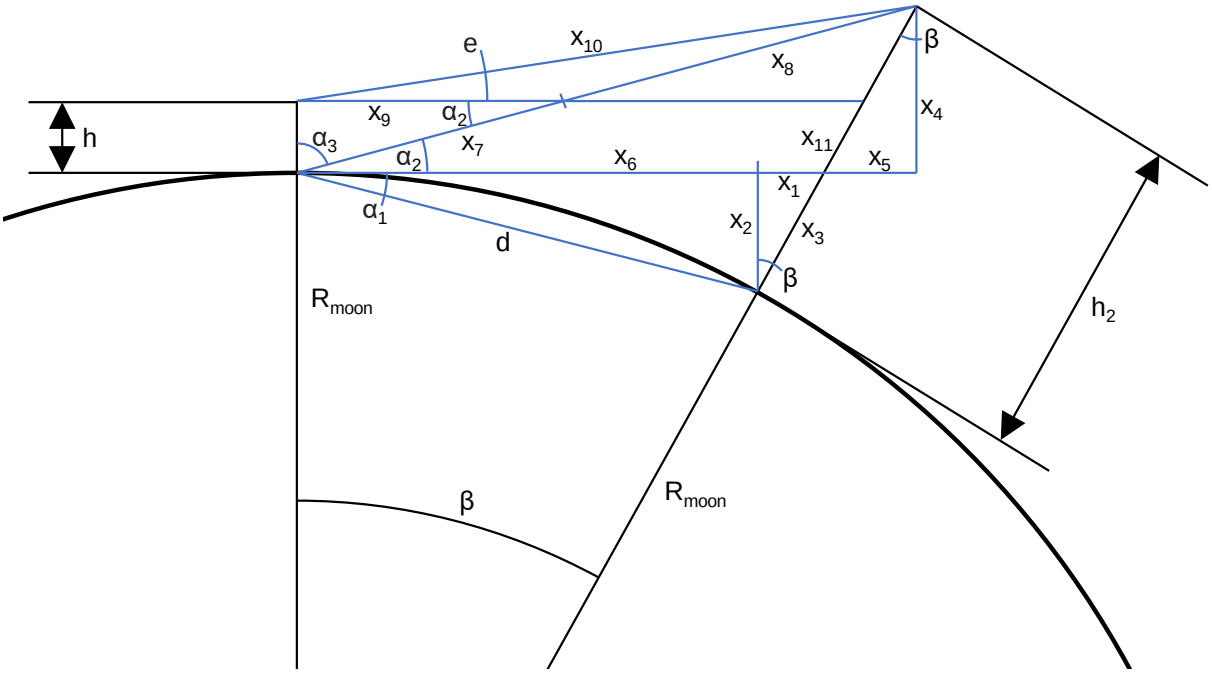

Fig. 2-5 Variables used in order to calculate the elevation angle e.

The script uses the variables shown in Fig. 2-5 to calculate the elevation angle between two pixels.

The following variables are known:

- the position of both pixels, the viewpoint and the observed point, from which their coordinates can be derived,
- the topographic heights h and h_2,
- and the mean radius of the Moon R_{Moon} used by the DEM data.

The calculation steps are shown in equation (2-1) to (2-17).

$$\beta = \cos^{-1}(\sin\theta_1 \cdot \sin\theta_2 + \cos\theta_1 \cdot \cos\theta_2 \cdot \cos(\lambda_2 - \lambda_1)) \qquad \textbf{(2-1)}$$

$$d = 2 \cdot \sin\frac{\beta}{2} \cdot R_{moon} \qquad \textbf{(2-2)}$$

$$\alpha_1 = \frac{\beta}{2} \qquad \textbf{(2-3)}$$

$$x_1 = \sin\alpha_1 \cdot d \quad \textbf{(2-4)}$$

$$x_2 = x_1 \cdot \tan\beta \quad \textbf{(2-5)}$$

$$x_3 = \frac{x_1}{\cos\beta} \quad \textbf{(2-6)}$$

$$x_4 = (h_2 - x_3) \cdot \cos\beta \quad \textbf{(2-7)}$$

$$x_5 = (h_2 - x_3) \cdot \sin\beta \quad \textbf{(2-8)}$$

$$x_6 = d \cdot \cos\alpha_1 \quad \textbf{(2-9)}$$

$$\alpha_2 = \tan^{-1}\frac{x_4}{x_2+x_5+x_6} \quad \textbf{(2-10)}$$

$$\alpha_3 = 90° - \alpha_2 \quad \textbf{(2-11)}$$

$$x_7 = \frac{h}{\cos\alpha_3} \quad \textbf{(2-12)}$$

$$x_8 = \sqrt{(x_2 + x_5 + x_6)^2 + {x_4}^2} - x_7 \quad \textbf{(2-13)}$$

$$x_9 = h \cdot \tan\alpha_3 \quad \textbf{(2-14)}$$

$$x_{10} = \sqrt{{x_8}^2 + {x_9}^2 - 2 \cdot x_8 \cdot x_9 \cdot \cos(180° - \alpha_2)} \quad \textbf{(2-15)}$$

$$x_{11} = \frac{h}{\cos\beta} \quad \textbf{(2-16)}$$

$$e = \cos^{-1}\frac{{x_9}^2+{x_{10}}^2-{x_8}^2}{2\cdot x_9\cdot x_{10}} \quad \textbf{(2-17)}$$

θ_1: *Latitude Viewpoint*

θ_2: *Latitude Observed Point*

λ_1: *Longitude Viewpoint*

λ_2: *Longitude Observed Point*

The script repeats the calculation of the elevation angle for every pixel (gray shading in Fig. 2-6) between the current location and the considered maximum viewing distance on the current azimuth angle. The highest angle found is used as the elevation angle for this azimuth angle. Repeating this process for every azimuth angle in 1° steps results in the complete local horizon for the current location in a resolution of 1°.

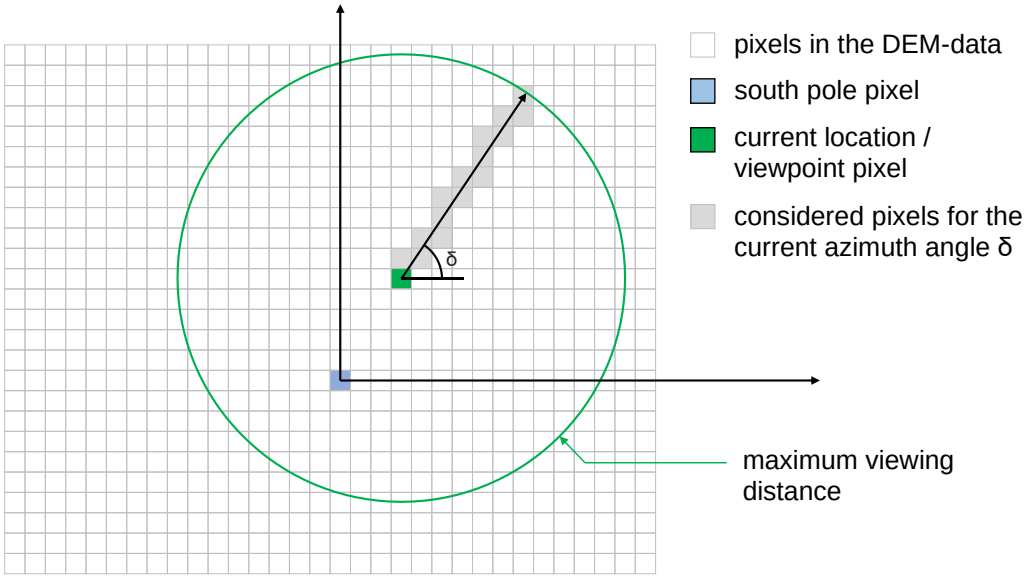

Fig. 2-6 Considered pixels for the currently looked at azimuth angle δ.

The maximum viewing distance used by the script is set by the closest map boundary. For a reliable result, the starting point should not be too close to the edge as the visual range on lunar mountains can be up to 200 km [5, p. 81]. This corresponds to a maximum latitude of -81.60° for the starting pixel for the DEM data used here. Any point further away from the south pole could lead to inaccurate results. All the considered landing regions in this paper are within this limitation.

The script also takes the viewpoint's height above the ground into account. This additional height was set to 2 m, as this is the same height used for exemplary horizon masks in a scientific paper by the California Institute of Technology from 2010. [16, p. 8]

In order to optimize the communication, the script now attempts to find the starting pixel inside the circular landing region which leads to the lowest local horizon with a stepwise calculation approach. Fig. 2-7 shows the script's process as a flowchart.

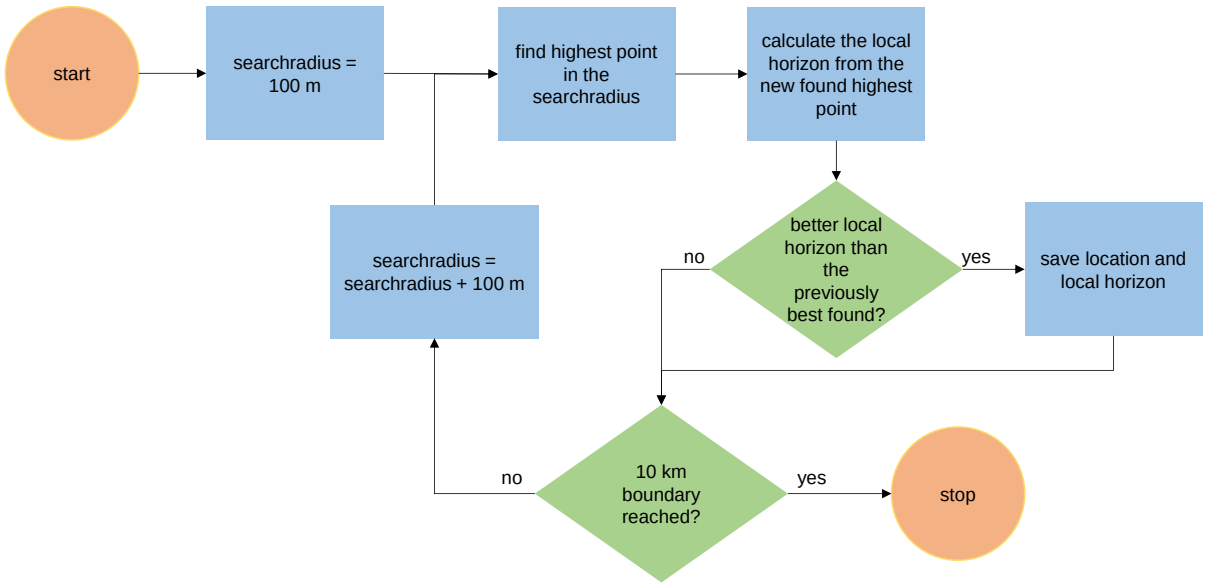

Fig. 2-7 Flowchart of the stepwise calculation approach used in “Local_Horizon.m” to find the position which allows optimal communication.

The script starts at the circle’s center, and begins to calculate the horizon, then it looks for the highest point within a 100 m radius and calculates the horizon again from that point. This process is repeated by increasing the search radius for the highest peak in 100 m steps until the boundary of the 10 km diameter landing region is reached. The point which has the lowest average elevation angle is then selected as the point with optimal communication (Fig. 2-7).

While this process takes a significantly longer time to calculate, it allows for more reliable results. Setting the point of best communication to the overall highest point in the region could lead to the point being on a hillside at the edge of the search radius, leading to an overall poorer azimuth elevation mask. The stepwise calculation allows for the detection of multiple smaller hills as local maxima in the terrain inside the landing region. It then compares the local horizon of each peak, selecting the one with the lowest local horizon. Fig. 2-8 shows the comparison between the local horizon of the overall highest point found in a 12.5 km search radius around region 102 (from Tab. 2-1) which ended up being on a hillside and the point with the best local horizon found by the stepwise calculation approach. The mean elevation angle across the azimuth range is -0.85° for the simple approach and -1.81° for the stepwise calculation.

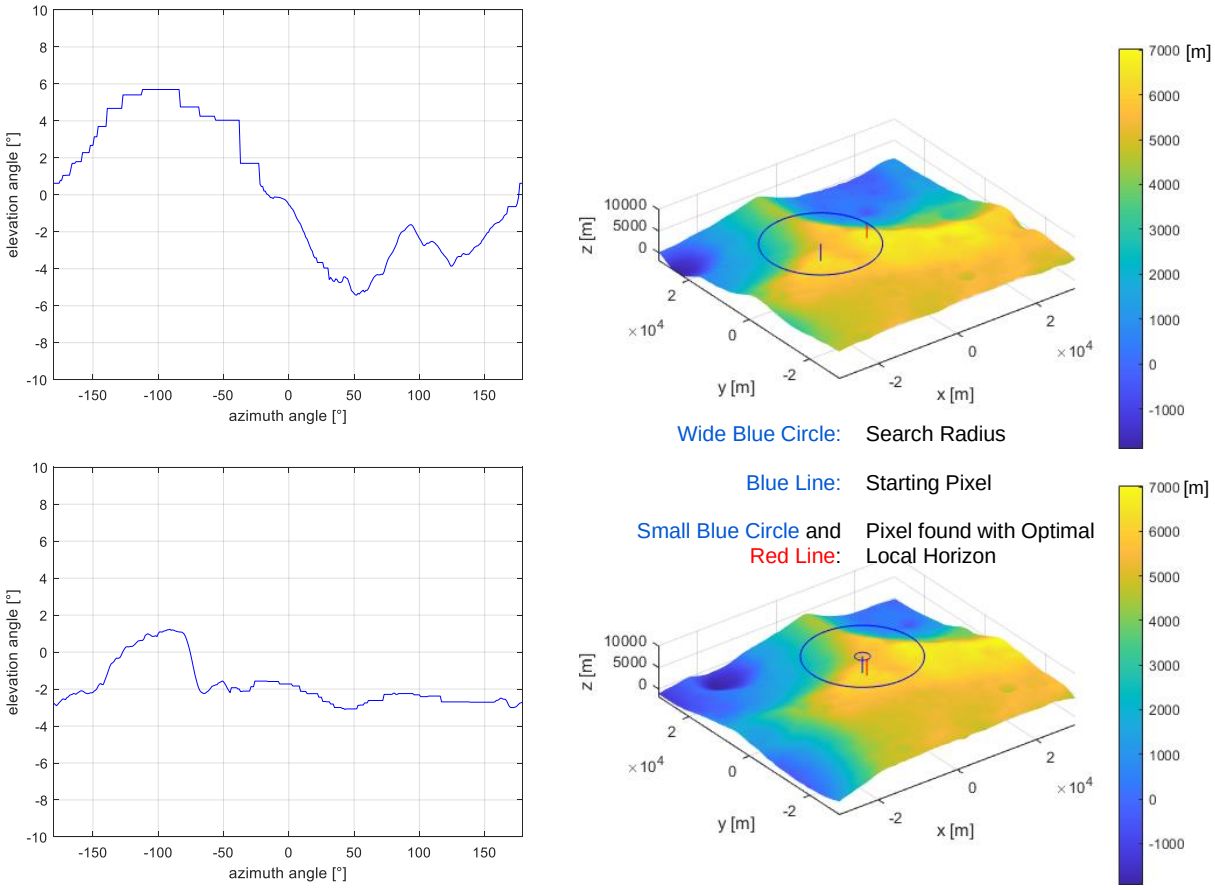

Fig. 2-8 Comparison of the azimuth elevation masks of the overall highest point in the search radius and the point found through the stepwise calculation (center at latiude: -89.4949 longitude: -119.0137 with a searchradius of 12.5 km).

2.2.2 Results

Using the stepwise calculation approach, the script determined the following coordinates for every landing region. The results are shown in Tab. 2-2 and in Fig. 2-9 to Fig. 2-15.

Tab. 2-2 Coordinates determined by the “Local_Horizon.m” script for optimal communication from the landing regions.

Landing Region	Optimal Latitude	Optimal Longitude
001	-89.4631°	-136.9415°
004	-89.8108°	-154.4400°
007	-88.8074°	123.7362°
011	-88.4492°	-67.9101°
102	-85.4035°	31.7121°
105	-87.1738°	61.0623°
Mount Kocher	-85.6805°	-116.6090°

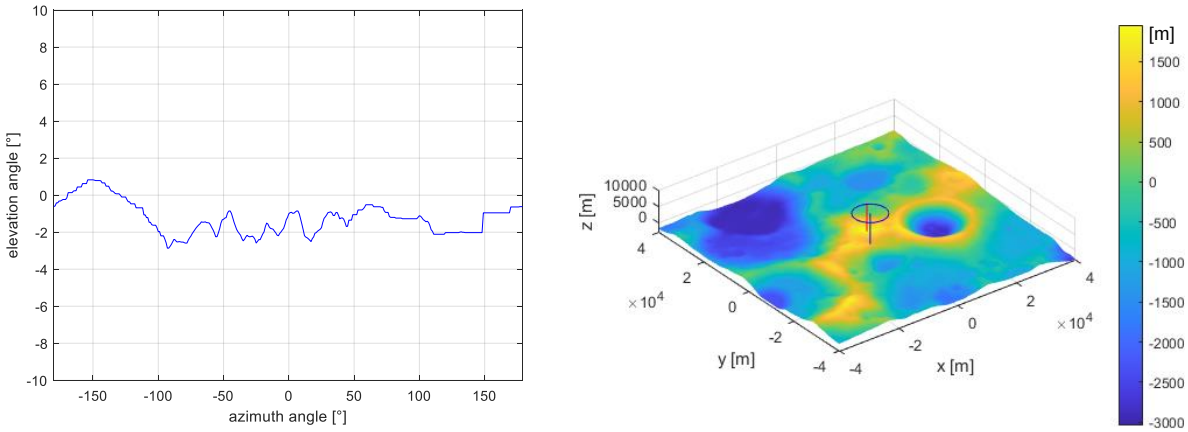

Fig. 2-9 Optimal local horizon of region 001 (latitude: 89.4631°, longitude: -136.9415°, additional height: 2 m). The azimuth angle 0° points north.

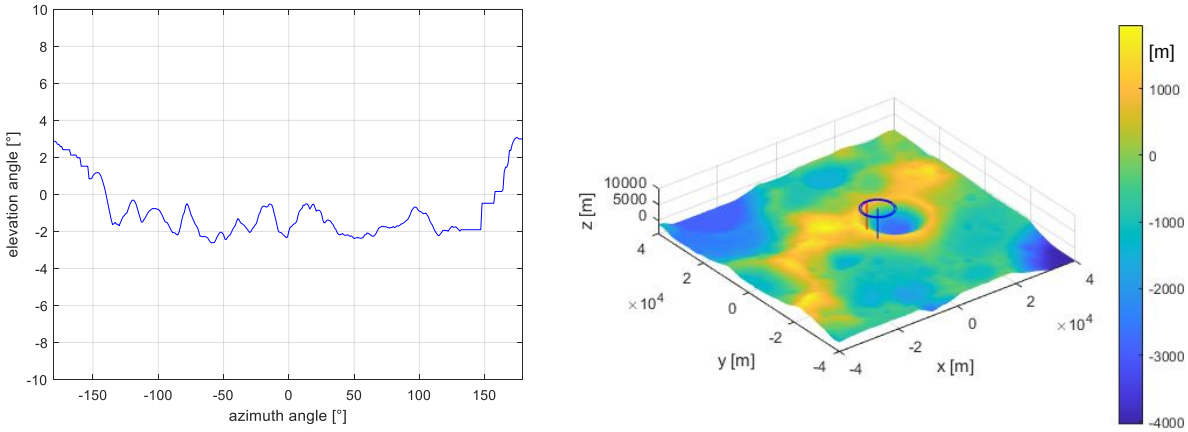

Fig. 2-10 Optimal local horizon of region 004 (latitude: -89.8108°, longitude: -154.4400°, additional height: 2 m).

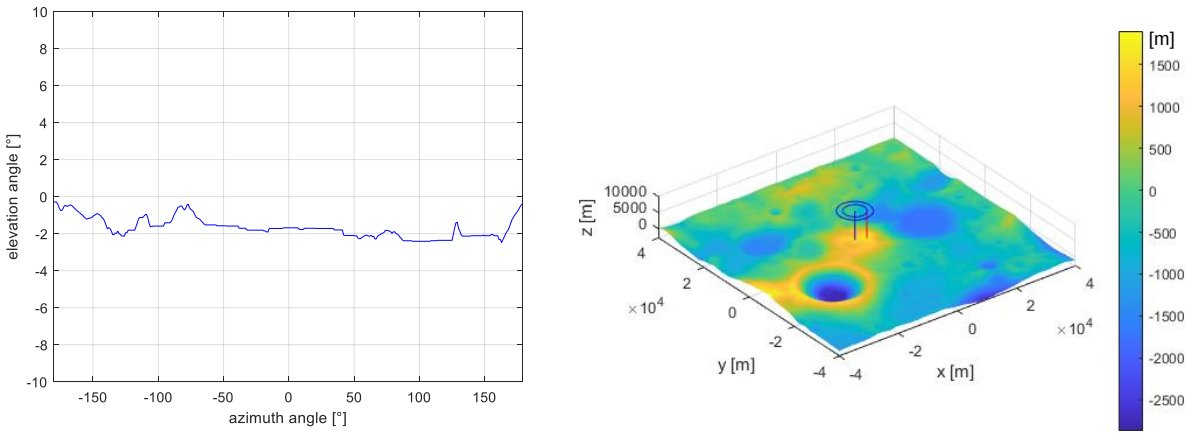

Fig. 2-11 Optimal local horizon of region 007 (latitude: -88.8074°, longitude: 123.7362°, additional height: 2 m).

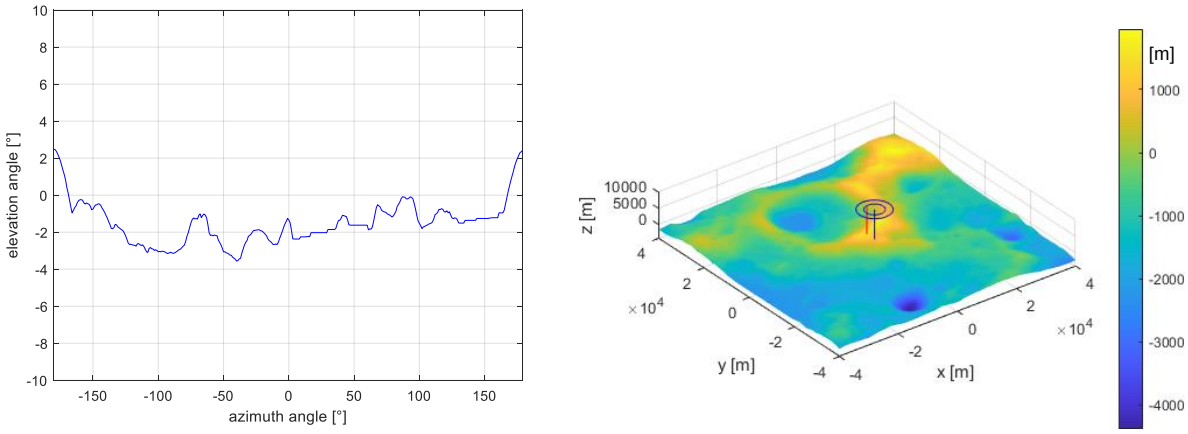

Fig. 2-12 Optimal local horizon of region 011 (latitude: -88.4492, longitude: -67.9101°, additional height: 2 m).

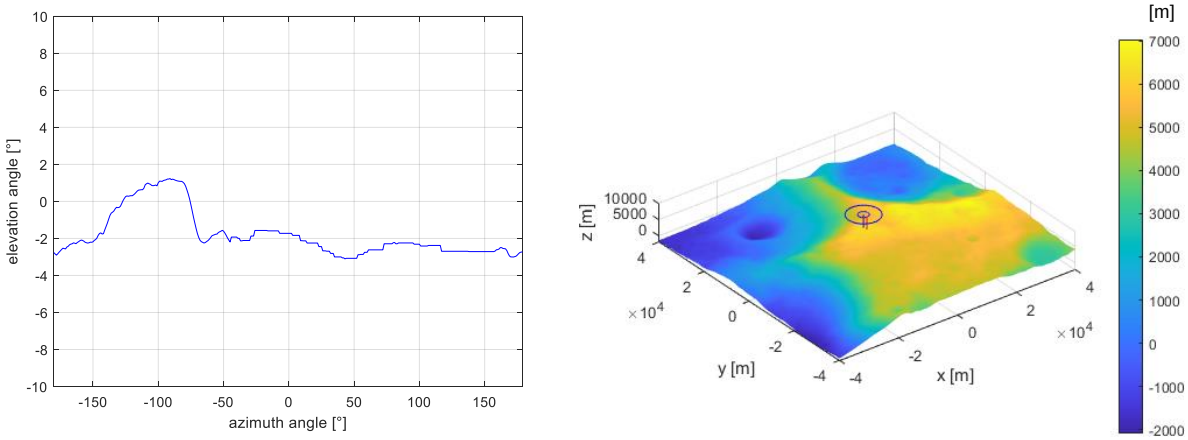

Fig. 2-13 Optimal local horizon of region 102 (latitude: -85.4035, longitude: 31.7121°, additional height: 2 m).

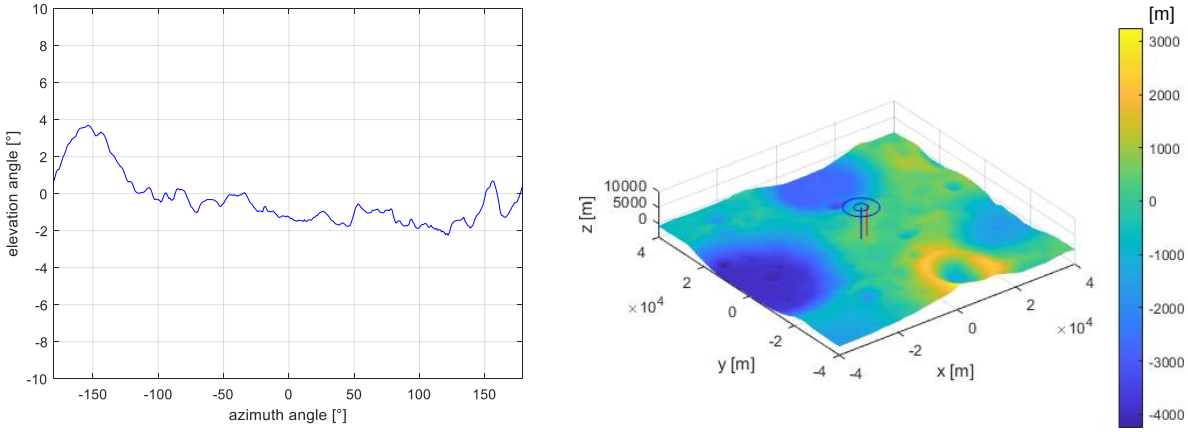

Fig. 2-14 Optimal local horizon of region 105 (latitude: -87.1738°, longitude: 61.0623°, additional height: 2 m).

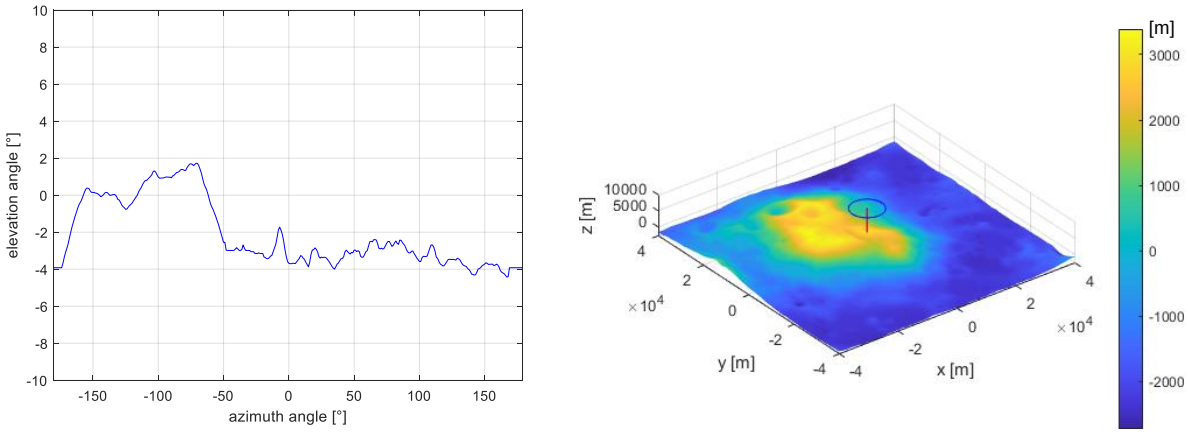

Fig. 2-15 Optimal local horizon of Mount Kocher (latitude: -85.6805°, longitude: -116.6090°, additional height: 2 m).

In Fig. 2-9 to Fig. 2-15 the azimuth angle 0° always points north. For the following communication analysis, the script also exports the azimuth elevation masks (AzEl-Masks) as .aem files. This file format can be used by AGI's System Tool Kit (STK) which in combination with MATLAB® will form the basis of the subsequent analysis.

3 Possible Communication Networks

3.1 Communication via Lunar Ground-Based Antenna Alone

3.1.1 Communication Directly from the Determined Landing Regions

The first humans might return to the Moon, landing near the south pole, while the lunar Gateway may still not be in service and other communication relay satellites have not yet been deployed. In contrast to the Apollo missions, which all landed on the near side of the Moon and could therefore ensure a constant radio communication with the Earth through a constant line-of-sight, landing sites near the lunar south pole may not have this advantage. Using the AzEl-Masks generated by the “Local_Horizon.m” script, a detailed communication analysis of the landing regions can be performed using STK.

As an additional comparison, the following analysis also considers the middle of the Shackleton crater as one of the viewpoints. The Shackleton crater is an impact crater located at the lunar south pole[2]. In the middle of the circular crater with an additional height of 2 m above the ground the crater walls result in a near constant elevation angle of about 20° (Tab. 3-1 and Fig. 3-1).

Tab. 3-1 Coordinates of the Shackleton Crater.

Landing Region	Latitude	Longitude
Shackleton	-89.63°	132.32°

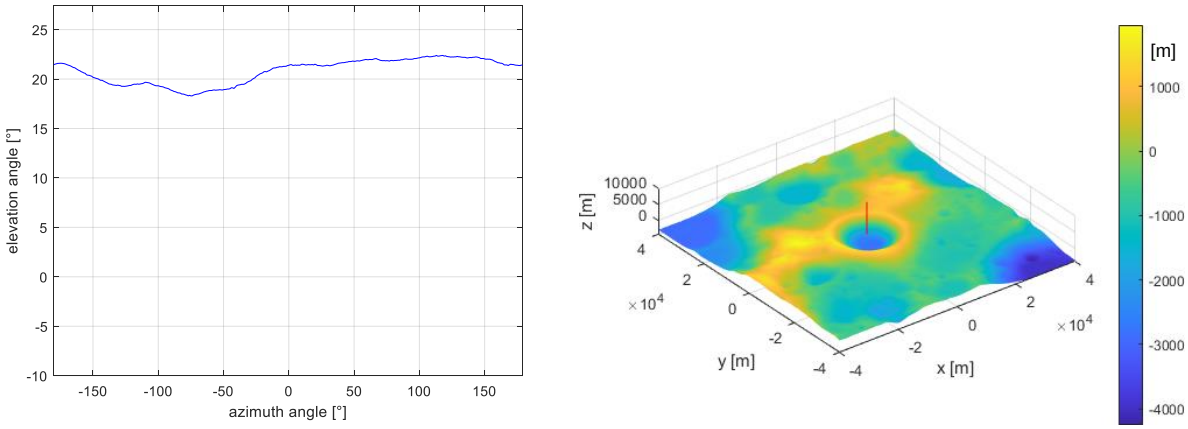

Fig. 3-1 Local horizon inside the Shackleton crater (latitude: -89.63°, longitude: 132.32°, additional height: 2 m). Determined by the “Local_Horizon.m” script with a search radius of 0 km.

The measured values for each landing region are:

- the coverage time [%],
- the maximum gap duration [h] during which no line-of-sight is present,
- the average gap duration [h] and
- the average number of gaps per year [-].

[2] The Shackleton crater is named after Sir Ernest Henry Shackleton who led three British expeditions to the Antarctic [17].

The following assumptions have been made for the scenario in STK to simulate the coverage:

- Communication between the Earth and the landing region can be achieved directly above the local horizon with an elevation angle of 0° above the horizon. This is possible because the Moon has no atmosphere allowing for unrestricted communication at low elevation angles.
- Communication can be achieved as soon as any line-of-sight with the Earth's surface can be attained. The simulation uses multiple facilities on the Earth's equator with coverage cones of 90° to simulate this.
- The scenario timeframe spans over one year from 01. Jan 2022 00:00:00.000 to 01. Jan 2023 00:00:00.000.

The results are shown in Tab. 3-2.

The scenario timeframes in this paper all span over approximately one year to cover at least one full rotation of the Earth-Moon-System around the Sun while ensuring a reasonable computing time. The simulation results would be more accurate with a longer scenario timeframe. This is due to the lunar precession which consists of the axial, apsidal and nodal precession. The lunar precessions have periods of 18.61 years for the axial and nodal precession and a period of 8.85 years for the apsidal precession [18, p. 7]. All the lunar precessions have an impact on the angle between the surface at the lunar south pole and the Earth. Only full simulations over a longer scenario timeframe would produce reliable results. Due to the limited available computing power, the lunar precession is neglected for this paper.

Tab. 3-2 Coverage results for direct contact from the landing regions.

Landing Region	Coverage Time [%]	Maximum Gap Duration [h]	Average Gap Duration [h]	Average Number of Gaps/Year [-]
001	61.26	248.34	82.77	41.03
004	61.49	246.10	78.46	43.03
007	59.07	261.90	100.90	34.02
011	64.67	230.36	81.45	38.03
102	100.00	0.00	0.00	0.00
105	65.23	224.65	67.69	45.03
Mount Kocher	56.56	278.34	130.98	28.02
Shackleton (for comparison)	49.43	325.35	142.36	29.02

All the potential landing regions show communication gaps which can last for multiple days except for region 102. This makes all landing regions except for 102 unsuitable for human missions without any additional communication network. Region 102 is located on a mountain allowing for a constant line-of-sight all year long. This makes for an optimal landing site for human missions to the lunar south pole without having to

install additional communication satellites into an orbit around the Moon first. Such landing sites are prime candidates for the return of humans to the Moon before building a more permanent presence. These first landings could be used to prove the technology needed to land on the lunar south pole. It is also possible that the permanently inhabited human base at the lunar south pole could be in one of these regions. From there, robotic assets could be deployed to other landing sites where other crews would land later. Those assets could be utilized temporarily while using the first landing site as a relay station for communication with the Earth. [19, p. 1]

3.1.2 Communication Directly from Local Mountain Peaks

3.1.2.1 Determining Suitable Regions

Like region 102 (from Tab. 3-2), other regions near the lunar south pole with a constant line-of-sight to the Earth would have to be mountain peaks. Their location should ideally be slightly on the near side of the Moon to enable full coverage during every state of the Moon's orbit even with its 5.14° inclination to ecliptic relative to the Earth (Fig. 3-2). [20]

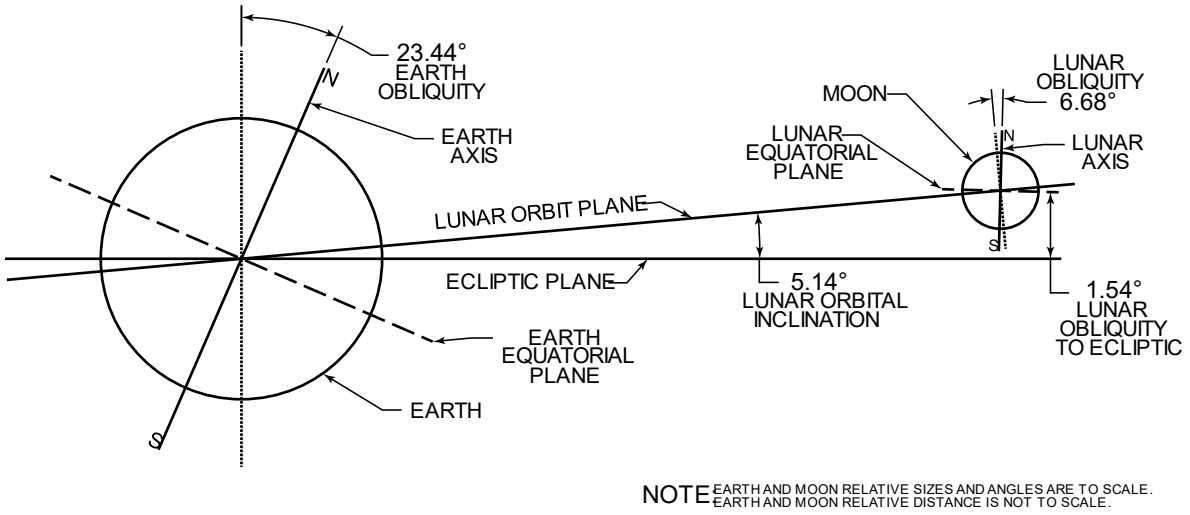

Fig. 3-2 Lunar orbit and orientation with respect to the ecliptic. The figure is taken from [21].

There are two mountains near the lunar south pole matching the criteria stated above. The Malapert Massif which includes region 102 and the Leibnitz Massif. Fig. 3-3 shows their location inside circles with a radius of 15 km and 25 km which include all the highest points of the plateaus. The coordinates of the circles' middle points can be determined to the numbers seen in Tab. 3-3. [22, p. 2]

Tab. 3-3 Coordinates of the Malapert and Leibnitz Massifs.

Landing Region	Latitude	Longitude
Malapert Massif	-84.9549°	38.1927°
Leibnitz Massif	-86.0316°	4.0207°

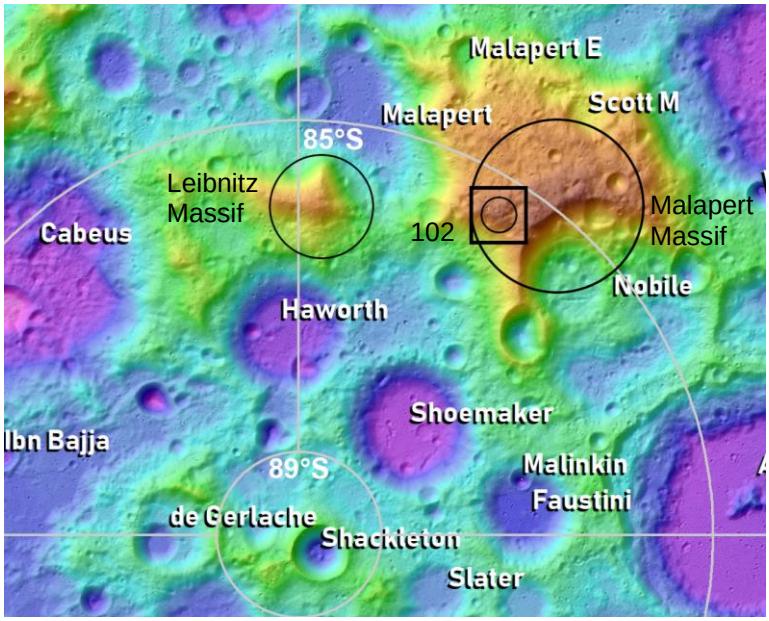

Fig. 3-3 The Leibnitz and Malapert Massifs near the lunar south pole inside circles with 15 km radius for Leibnitz and 25 km radius for Malapert. The black circles and quadrats are added to the Topographic Map of the Moon's South Pole taken from [12].

3.1.2.2 Communication from the Malapert and Leibnitz Massif

In order to analyze the communication between the two mountains and the Earth, the "Local_Horizon.m" script uses a search radius of 25 km for the Malapert and 15 km for the Leibnitz Massif, as shown in Fig. 3-3 with a 100 m step size to find the location with the best local horizon. The script determined the following coordinates (Tab. 3-4 and Fig. 3-4).

Tab. 3-4 Coordinates determined by the "Local_Horizon.m" script for optimal communication from the Malapert Massif.

Landing Region	Latitude	Longitude
Malapert Massif	-84.8344°	38.2616°
Leibnitz Massif	-85.9887°	2.0840°

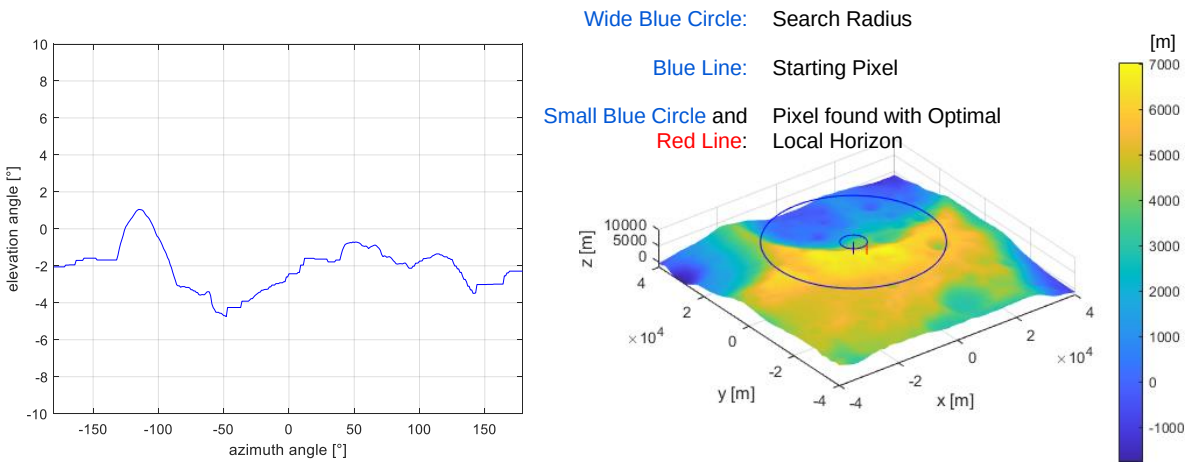

Fig. 3-4 Optimal local horizon of the Malapert Massif (latitude: -84.8344°, longitude: 38.2616°, additional height: 2 m).

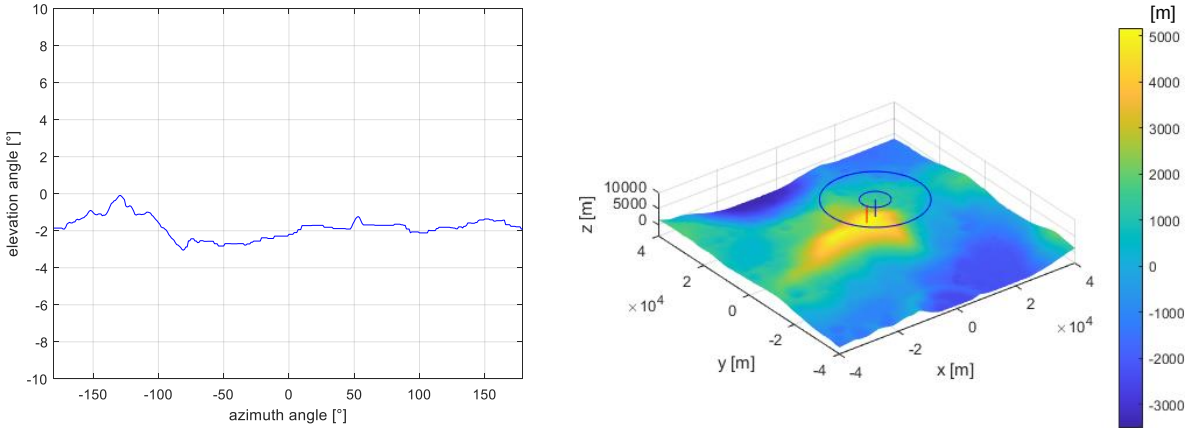

Fig. 3-5 Optimal local horizon of the Leibnitz Massif (latitude: -85.9887°, longitude: 2.0840°, additional height: 2 m).

Using the same assumptions for the STK coverage simulation as for the landing regions in 3.1.1, the results show a 100% coverage between the Earth and both mountains (Tab. 3-5).

Tab. 3-5 Coverage results for direct contact from the Malapert and Leibnitz Massifs with Earth's facilities on the equator.

Landing Region	Coverage Time [%]	Maximum Gap Duration [h]	Average Gap Duration [h]	Average Number of Gaps/Year [-]
Malapert Massif	100.00	0.00	0.00	0.00
Leibnitz Massif	100.00	0.00	0.00	0.00

The MATLAB® script “STK_Direct_Contact_Simulation.m” changes the latitudes of the facilities placed on the Earth in 10° steps to show the range in which the antenna on the Earth can be placed while still achieving a 100% coverage. This is done to determine whether the Earth always fully rises above the horizon when observed from the two massifs or whether the ground stations on the Earth would have to be placed along certain latitudes. The script places all Earth-bound facilities on the same latitude across the longitudes and then varies this latitude. The coverage results are shown in Tab. 3-6.

Tab. 3-6 Coverage time of Malapert and Leibnitz with Earth facilities on different latitudes.

Latitude of Earth Facilities [°]	Coverage Time Malapert [%]	Coverage Time Leibnitz [%]
-90	46.66	46.66
-80	58.09	58.09
-70	71.28	71.28
-60	93.96	93.96
-50	100.00	100.00
-40	100.00	100.00
-30	100.00	100.00
-20	100.00	100.00
-10	100.00	100.00
0	100.00	100.00
10	100.00	100.00
20	100.00	100.00
30	100.00	100.00
40	100.00	100.00
50	100.00	100.00
60	93.59	93.59
70	73.98	73.98
80	62.10	62.10
90	51.00	51.00

The values between the two sites are almost identical. Fig. 3-6 shows the visualization of Malapert’s data from Tab. 3-6.

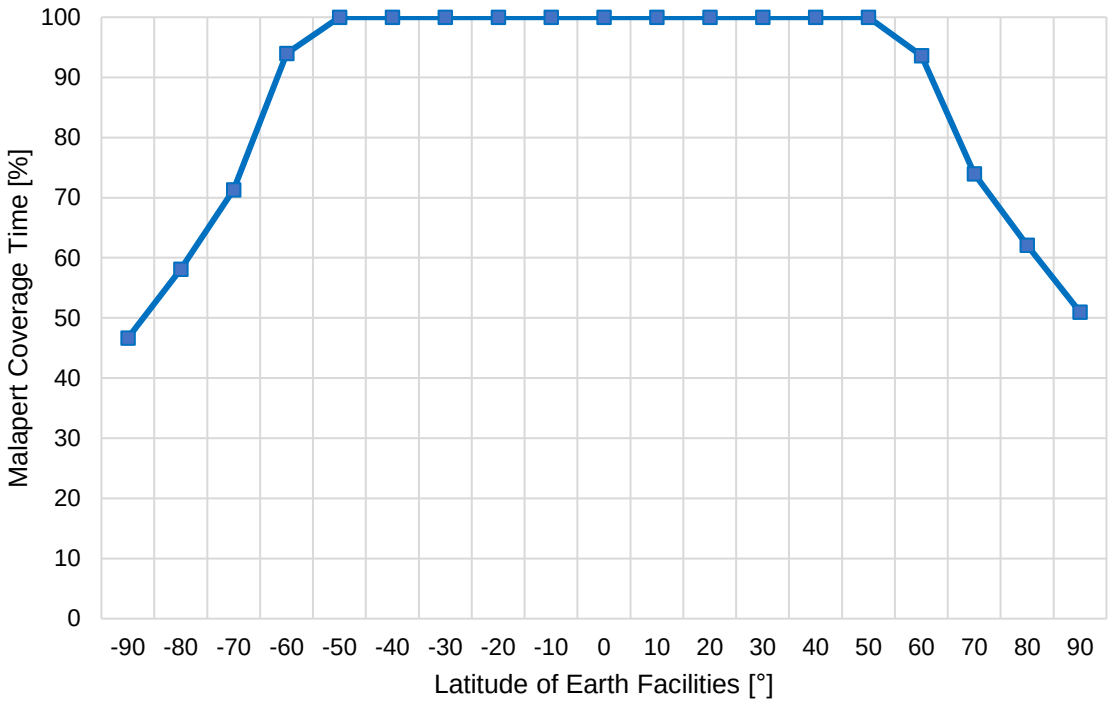

Fig. 3-6 Graph of the Coverage Time of Malapert with Earth facilities on different latitudes.

The simulation shows that the antenna on the surface of the Earth that communicate with the Malapert and Leibnitz regions can be placed anywhere between -50° and 50° latitude on the Earth. Within these limitations, both the Malapert and the Leibnitz Massif have been determined to allow full coverage over the entire scenario timeframe without any additional satellites functioning as signal relays. This makes them prime candidates for landing sites in the early phases of returning to the Moon.

3.2 Communication via a Relay Satellite Constellation

3.2.1 Approach to Identify Optimal Constellations

A relay satellite constellation around the Moon allows for a more flexible selection of landing sites at the lunar south pole as they do not depend on a direct line-of-sight to the Earth. The landing sites can communicate with the ground stations on the Earth via one or multiple relay satellites which can receive and forward signals.

For the following analysis, the MATLAB® script “STK_Constellation_Simulation.m” was written within the scope of this paper. It provides an interface to STK and simulates multiple possible constellations of satellites around the Moon. It then calculates values for each constellation which allow the evaluation of the communication with the potential landing regions selected in 2.2.2.

The measured values for each landing region and each constellation are:

- the coverage time [%],
- the maximum gap duration [h] during which no contact is present,
- the average gap duration [h],
- the average number of gaps per year [-] and

- the average number of assets (satellites) available/viewable [-].

For a better comparison between the constellations, these values are first calculated for every landing region and are then averaged to mean values of all regions.

Additionally, for each simulated constellation the script also calculates the coverage time [%] of landing sites placed along the 180° longitude line on the Moon which runs along the middle of the far side of the Moon. This enables the comparison of additional values:

- the coverage time of the north pole [%],
- an approximation of the average far side coverage [%] and
- the maximum far side coverage [%] somewhere on the far side of the Moon between the latitudes -80° and 80°.

The average far side coverage expresses the mean portion of the total far side of the Moon which is covered by the constellation during the entire scenario timeframe. It is calculated by factorizing the values along the 180° longitude with the surface portion they represent on the Moon's spherical surface. The facilities are placed along the far side in 10° latitude from -90° to 90°. The maximum far side coverage shows the maximum coverage achievable somewhere on the far side of the Moon someplace between the latitudes -80° and 80°. As deep space observation is not bound to a specific region on the far side, it would be enabled if sufficient coverage is achieved anywhere in that region.

The following assumptions have been made for the scenario in STK to simulate the coverage:

- Communication between the landing regions and the satellites can be achieved directly above the local horizon. This means, it is possible at an elevation angle of 0° above the lunar horizon as the Moon has no atmosphere allowing for unrestricted communication at low elevation angles.
- Communication can be achieved as soon as any line-of-sight with the Earth's surface can be attained. The simulation uses multiple facilities on the Earth's equator with coverage cones of 90° to simulate this.
- The scenario timeframe spans over one year from 01. Jan 2022 00:00:00.000 to 01. Jan 2023 00:00:00.000.

Throughout this paper the orbital information of satellites will be expressed via the six known orbital elements (Fig. 3-7).

- apoapsis height
- periapsis height
- inclination
- longitude of the ascending node
- argument of periapsis
- true anomaly

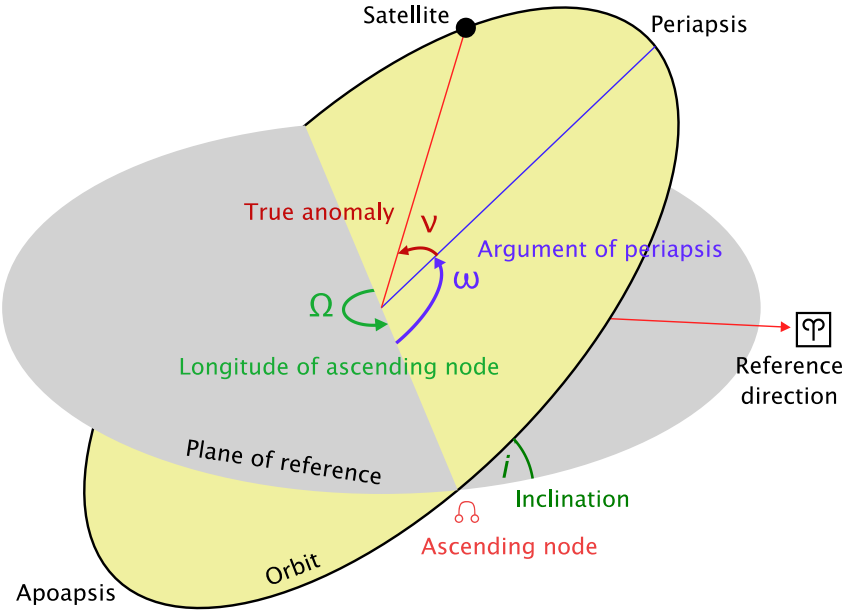

Fig. 3-7 Orbital elements. The additional labels for apoapsis and periapsis were added to the figure taken from [23].

3.2.2 Polar Circular Orbits

The first kind of constellations simulated by the MATLAB® script "STK_Constellation_Simulation.m" are polar circular orbit constellations. The orbits in such a constellation are characterized by an inclination of 90° as well as an eccentricity of 0, which means that the periapsis and apoapsis are the same and therefore the orbits are circular rather than elliptical. Since the orbits are circular, the argument of periapsis has no influence on the orbits. Also, the longitude of the ascending node will have no influence on the results as the target area is located at one of the poles and the Moon rotates underneath the satellites' orbits over the timeframe of the simulation. The true anomaly describes the position of the satellite on its orbit at a specific moment. With only one satellite, the true anomaly set at the beginning of the scenario has no influence on the results. When using multiple satellites, the true anomalies at the beginning of the scenario will be set so as that the satellites are evenly distributed. This leaves only the periapsis/apoapsis height as variable parameter.

Fig. 3-8 shows the coverage time [%] as well as the maximum communication gap duration [h] averaged over all potential landing sites achieved by one relay satellite in a polar circular orbit while varying the apoapsis/periapsis height along the x-axis. It shows that a higher orbit leads to longer but fewer communication gaps while the coverage time approaches 50% with increasing orbit height. As the orbit is circular with an inclination larger than 0, the satellite spends half its time above the northern hemisphere and the other half above the southern hemisphere. The higher the orbit, the sooner a contact between the south pole and the satellite can be established with respect to its true anomaly or relative position on its orbit. Therefore, the maximum achievable coverage time with one polar circular satellite cannot exceed 50%. In Fig. 3-8 the coverage time of the highest orbit is slightly higher than 50%. This is due to the fact that the satellite's true anomaly was set to be directly above the south pole at the beginning of the scenario. At the end of the scenario, the satellite was once again

above the southern hemisphere. The scenario timeframe of one year was not long enough to adjust this proportionally longer stay above the southern hemisphere.

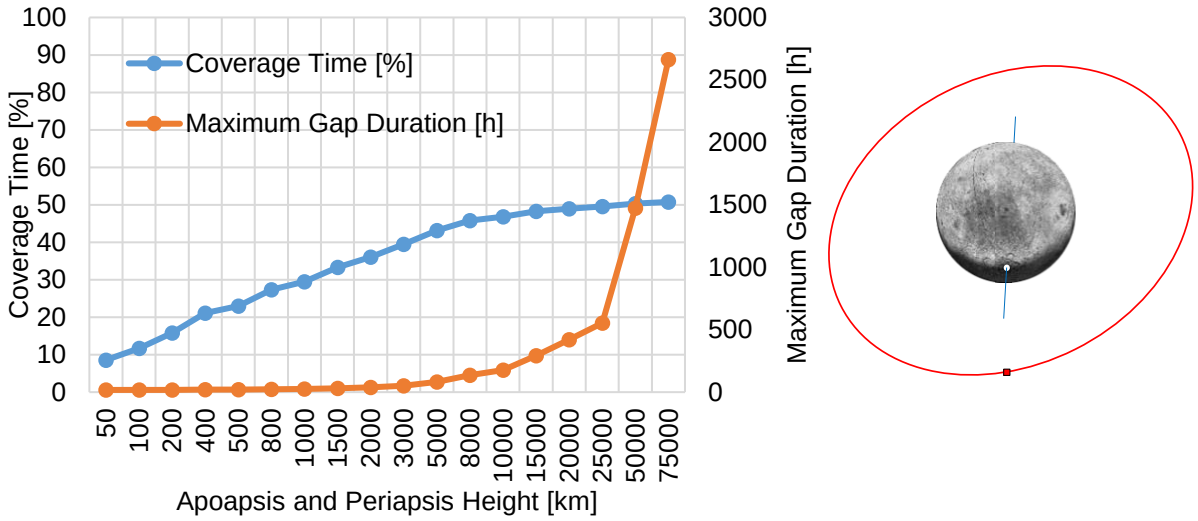

Fig. 3-8 Coverage time and maximum communication gap duration averaged over the potential landing sites at the lunar south pole provided by one relay satellite in a polar circular orbit.

In a next step, the script places a second satellite in a circular polar orbit with opposing true anomalies at the start so as that the satellites are always opposite of each other. Fig. 3-9 shows the coverage time and maximum gap duration averaged over all potential landing sites while varying the orbit height. The graph shows similar trends to the simulation with just one satellite. Here, the coverage time approaches but never reaches 100% with increasing orbit height, while the maximum gap duration increases but the number of gaps decreases. The two opposing circular satellites can never achieve a 100% coverage, because there will always be a moment where both satellites are directly above the equator simultaneously. In this position, no contact between the south pole and the relay satellites can be achieved.

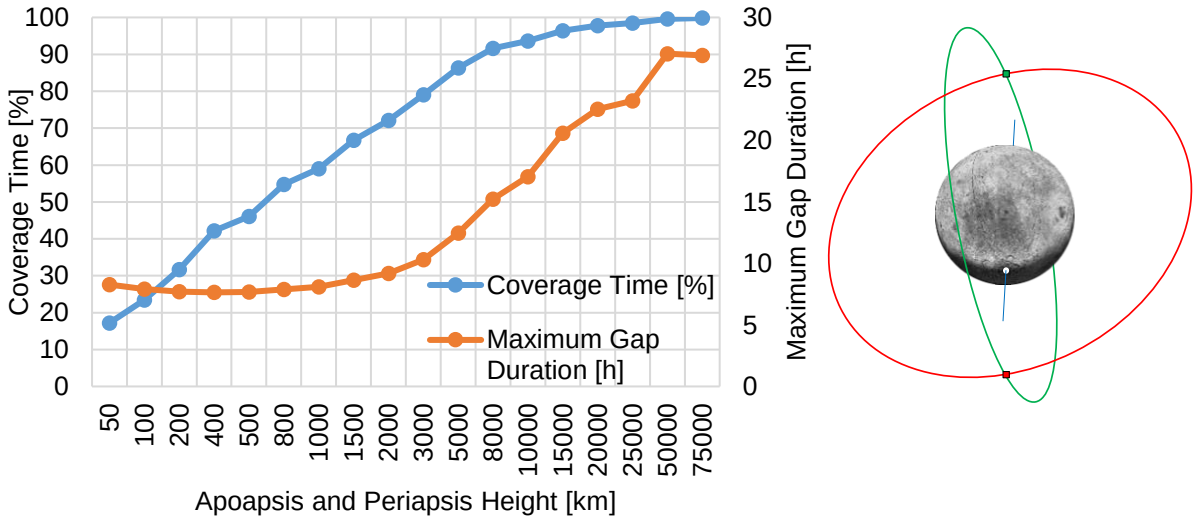

Fig. 3-9 Coverage time and maximum communication gap duration averaged over the potential landing sites at the lunar south pole provided by two opposing relay satellites in polar circular orbits with the same orbit heights.

Fig. 3-10 shows the same simulation with an additional third satellite. The three satellites are evenly distributed along their orbits. The graph shows that at an apoapsis and periapsis height of 3000 km and higher a 100% coverage time with zero communication gaps for all potential landing sites is achieved.

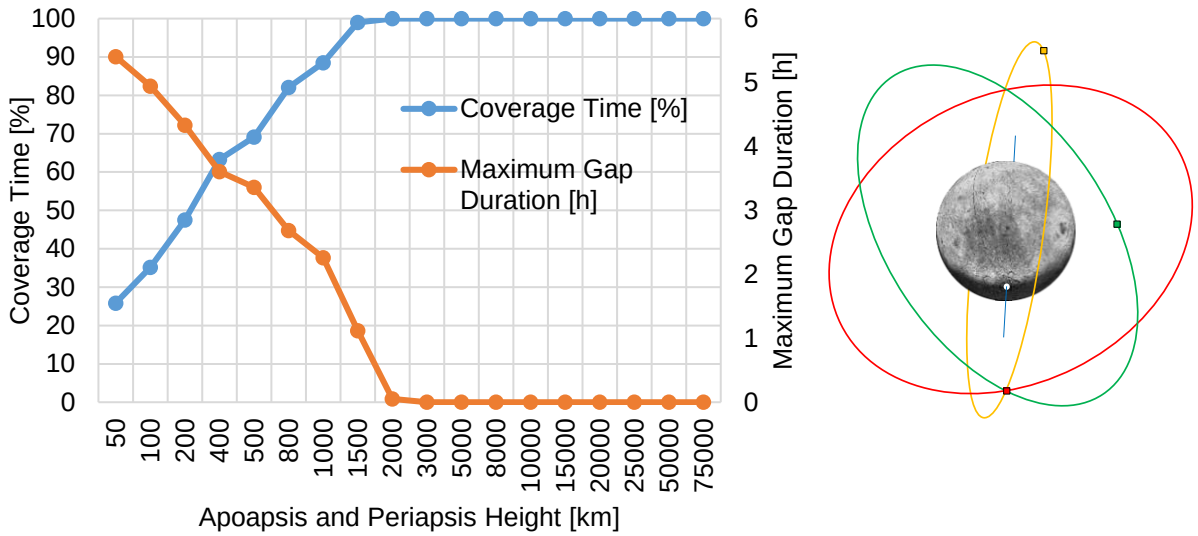

Fig. 3-10 Coverage time and maximum communication gap duration averaged over the potential landing sites at the lunar south pole provided by three evenly distributed relay satellites in polar circular orbits with the same orbit heights.

3.2.3 Inclined Circular Orbits

Inclined circular orbits are characterized by an eccentricity of 0 but contrary to polar circular orbits, the inclination is variable. The MATLAB® script takes the three-satellite-constellation shown in 3.2.2 and varies the inclination of all three orbital planes. Fig. 3-11 shows the results of this analysis. For an inclination of 70° to 110° the constellation with an apoapsis and periapsis height of 3000 km achieves a 100% coverage time with zero gaps.

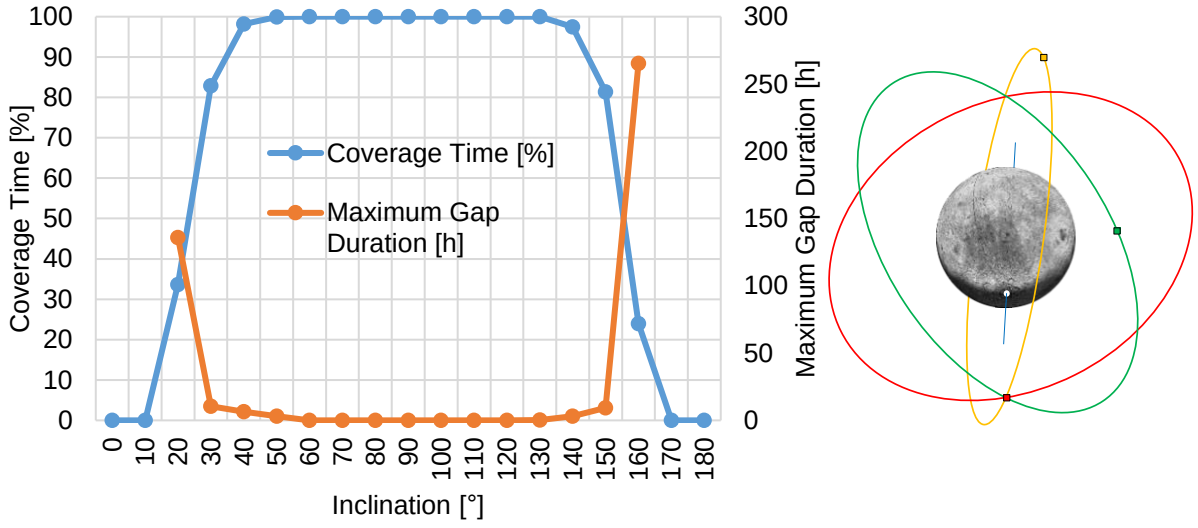

Fig. 3-11 Influence of the inclination on the south pole coverage for a three-satellite-circular-constellation with an apoapsis and periapsis height of 3000 km.

Fig. 3-12 shows the average number of assets (satellites) available at any time averaged over the potential landing sites. This means it shows the number of the satellites in reach averaged over the entire scenario timeframe. As expected, the peak at 90° shows that for targets near the poles an inclination of 90° provides the best satellite contact. At inclinations of 0° or 180°, the satellites orbit only above the equator and therefore no coverage of the poles is provided.

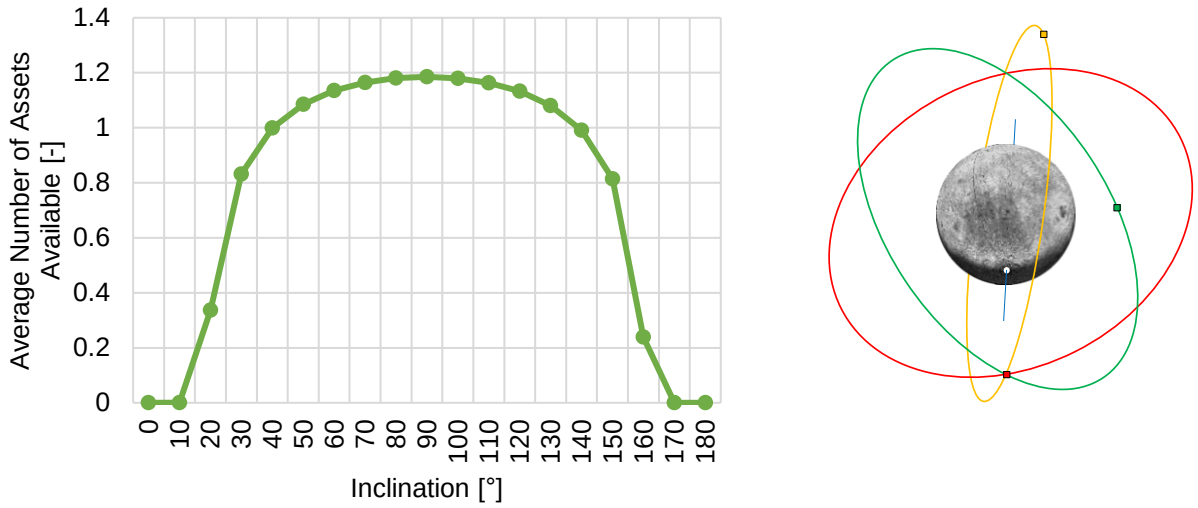

Fig. 3-12 Influence of the inclination on the average number of assets available at the south pole for a three-satellite-circular-constellation with an apoapsis and periapsis height of 3000 km. The peak is achieved at an inclination of 90°.

This shows that at least three satellites are needed to achieve a 100% coverage of the potential landing sites when only using circular orbits. But as the orbits are symmetric to the equatorial plane, the same coverage of 100% is achieved at the north pole.

3.2.4 Elliptical Orbits

Unlike inclined circular orbits, elliptical orbits are not characterized by an eccentricity of 0 which means that they can have an elliptical shape with a different apoapsis and periapsis height. This allows for a multitude of different constellations. To evaluate the different constellations and find the most suitable one, a score system is applied. The measured values selected for the score calculation are:

- the maximum gap duration [h] during which no line-of-sight is present,
- the coverage time of the north pole [%],
- the average far side coverage [%] and
- the maximum far side coverage [%] somewhere on the far side of the Moon between the latitudes -80° and 80°.

The score calculation is shown in equation (3-1) and reaches from 0 to 100. If the maximum gap duration is larger than the set maximum allowed gap duration, the score is automatically 0.

$$s = \frac{\left(\left(1-\frac{t_{Gap}}{t_{GapAllowed}}\right)\cdot w_{Gap}\cdot 100 + c_{Sha}\cdot w_{Sha} + c_{NP}\cdot w_{NP} + c_{AFS}\cdot w_{AFS} + c_{MFS}\cdot w_{MFS}\right)}{w_{Gap}+w_{Sha}+w_{NP}+w_{AFS}+w_{MFS}} \quad \textbf{(3-1)}$$

t_{Gap}: $Maximum\ Gap\ Duration\ [s]$

$t_{GapAllowed}$: $Maximum\ Allowed\ Gap\ Duration\ [s]$

c_{Sha}: $Coverage\ inside\ the\ Shackleton\ Crater\ [\%]$

c_{NP}: $North\ Pole\ Coverage\ [\%]$

c_{AFS}: $Average\ Far\ Side\ Coverage\ [\%]$

c_{MFS}: $Maximum\ Far\ Side\ Coverage\ [\%]$

w_{Gap}: $Weighting\ of\ Gap\ Duration\ score$ [-]

w_{Sha}: $Weighting\ of\ Shackleton\ Coverage\ score$ [-]

w_{NP}: $Weighting\ of\ North\ Pole\ Coverage\ score$ [-]

w_{AFS}: $Weighting\ of\ Average\ Far\ Side\ Coverage\ score$ [-]

w_{MFS}: $Weighting\ of\ Maximum\ Far\ Side\ Coverage\ score$ [-]

The following weightings and times were set according to their importance (3-2) to (3-7).

$$t_{GapAllowed} = 600\ s \quad \textbf{(3-2)}$$

$$w_{Gap} = 1 \quad \textbf{(3-3)}$$

$$w_{Sha} = 0.5 \quad \textbf{(3-4)}$$

$$w_{NP} = 0.3 \quad \textbf{(3-5)}$$

$$w_{AFS} = 0.15 \quad \textbf{(3-6)}$$

$$w_{MFS} = 0.3 \quad \textbf{(3-7)}$$

The elliptical shape of the orbits results in a lower orbital velocity at the apoapsis and a higher one at the periapsis. Placing an orbit's apoapsis above the south pole can therefore result in a satellite's visibility from the south pole of more than 50%, which is the upper theoretical limit for circular orbits. Only two satellites on the same elliptical orbit with an apoapsis above the south pole can therefore reach a 100% coverage at the south pole. Next, the MATLAB® script evaluates the impact of the argument of periapsis of two satellites with the same eccentricity and semimajor axis. It moves the argument of periapsis in 22.5° steps and evaluates the score achieved by every possible combination of two orbits with different or same arguments of periapsis. The satellite's true anomaly is set so as that they always reach the opposing poles at the same time (Fig. 3-13). The best scoring results of varying the argument of periapsis are shown in Tab. 3-7.

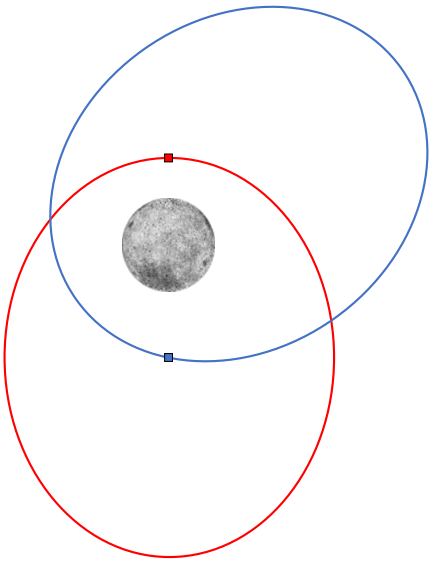

Fig. 3-13 Two elliptical orbits with different arguments of periapsis. The eccentricity, semimajor axis, ascending node and inclination are identical.

Tab. 3-7 Best scoring results of varying the argument of periapsis in 22.5° steps of two otherwise identical orbits.

Argument of Periapsis 1 [°]	Argument of Periapsis 2 [°]	Apoapsis Height [km]	Periapsis Height [km]	Inclination [°]	Mean Coverage Time [%]	Mean Maximum Gap Duration [s]	North Pole Coverage [%]	Average Far Side Coverage [%]	Maximum Far Side Coverage [%]	Score [-]
45	180	10000	1500	90	100	0	56.42	73.44	99.88	92.40
135	0	10000	1500	90	100	0	56.36	73.17	99.78	92.36
157.5	22.5	10000	1500	90	99.99998	1.51	50.67	73.30	99.93	91.52
22.5	157.5	10000	1500	90	99.99996	3.90	50.69	73.27	99.93	91.34
112.5	0	10000	1500	90	100	0	51.70	68.52	98.89	91.31
45	157.5	10000	1500	90	100	0	40.93	70.89	99.999 996	90.18

The constellations with the highest score are all displaying a difference of over 100° between the two arguments of periapsis. This suggests that a larger difference in the argument of periapsis can still achieve a 100% coverage of the south pole region while also providing relatively good coverage of the north pole and far side regions.

However, setting the arguments of periapsis directly over the poles with a difference of 180° does not achieve a 100% coverage at any pole. This is due to the fact that the orbits in this calculation have the same periapsis and apoapsis heights, which would lead to symmetrical movement with respect to the lunar equatorial plane. This leads to moments when both satellites are exactly above the equator simultaneously and are therefore unable to connect to any of the polar regions. This problem should be avoidable if one of the orbits has a different eccentricity while retaining the same orbit period. The difference between these two constellations is shown in Fig. 3-14.

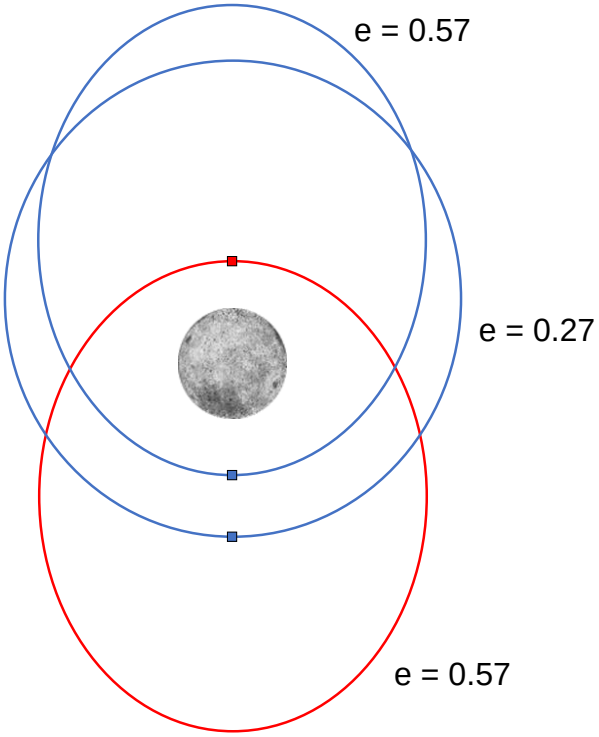

Fig. 3-14 Varying the eccentricity of one of the elliptical orbits with opposing arguments of periapsis while retaining the same orbit period.

Tab. 3-8 shows the results for the two combinations shown in Fig. 3-14. The constellation of two orbits with the same eccentricity of 0.57 results in a maximum communication gap at the south pole of more than 11h and therefore a score of 0. But it also shows a tremendously better north pole coverage of 87.47%. Lowering the eccentricity of the orbit which has its argument of periapsis set above the south pole to 0.27 results in a full south pole coverage while still achieving a higher score than any of the scores achieved by two orbits with the same eccentricity.

Tab. 3-8 Coverage results of the two constellations shown in Fig. 3-14.

Argument of Periapsis 1 [°]	Argument of Periapsis 2 [°]	Semimajor Axis [km]	Eccentricity 1 [-]	Eccentricity 2 [-]	Inclination [°]	Mean Coverage Time [%]	Mean Maximum Gap Duration [h]	North Pole Coverage [%]	Average Far Side Coverage [%]	Maximum Far Side Coverage [%]	Score [-]
90	270	7487.4	0.57	0.57	90	89.17	11.32	87.47	74.82	86.96	0.00
90	270	7487.4	0.57	0.27	90	100	0	69.17	74.67	99.87	94.18

There are infinite possibilities of orbit combinations with this elliptical constellation type. The MATLAB® script is not capable of simulating a sufficient number of constellations in a reasonable time to find the best possible combination. It would be necessary to set one of the satellites on a fixed orbit and simulate the other one to find the best matching orbits resulting in the highest score. The Lunar Gateway is planned to be set on a similar elliptical orbit around the Moon with an apoapsis high above the south pole. It will be capable of receiving and forwarding signals and can therefore be used as a relay node. For this paper, the Gateway in its highly elliptical orbit will be used in the constellation simulation. In the following chapters, the MATLAB® script will simulate different satellites to identify the best additional satellite to the Gateway resulting in the highest score.

3.3 Communication to the Landing Regions via the Lunar Gateway

3.3.1 The Lunar Gateway's Near-Rectilinear Halo Orbit

The Lunar Gateway's Near-Rectilinear Halo Orbit (NRHO) will be a L2 southern halo in a 9:2 resonance with the lunar synodic period. This results in an orbit period of approximately 6.5 days. The orbit is highly elliptical with a periapsis height of about 1,500 km above the lunar north pole and an apoapsis above the south pole with a height of about 70,000 km. [24, p. 1]

Halo orbits allow for the ascending node of the orbit to rotate throughout the orbit period. In the Gateway's case, the rotation relative to the center of the Moon allows for a constant line-of-sight to the Earth while the Moon orbits the Earth as the Gateway is

never positioned behind the Moon. This allows for constant communication between the Earth and the Gateway. As the Gateway's apoapsis is high above the south pole, it remains visible for landing sites there and stays high above the horizon for the majority of the Gateway's orbit. This makes the Gateway a suitable relay node in the communication between the Earth and the potential landing regions at the lunar south pole. The following calculations will analyze this. Fig. 3-15 shows the NRHO as seen from different reference frames. The Earth-Moon rotating system shows the view from the Earth and how the Gateway always stays visible throughout its orbit.

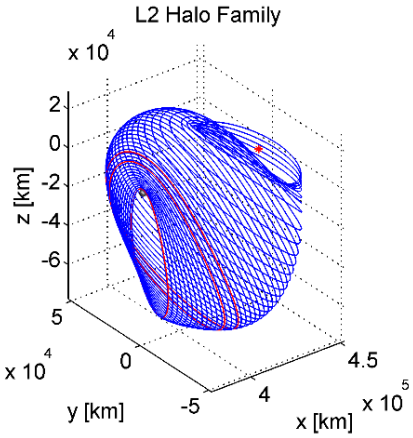

In the Earth-Moon rotating system.

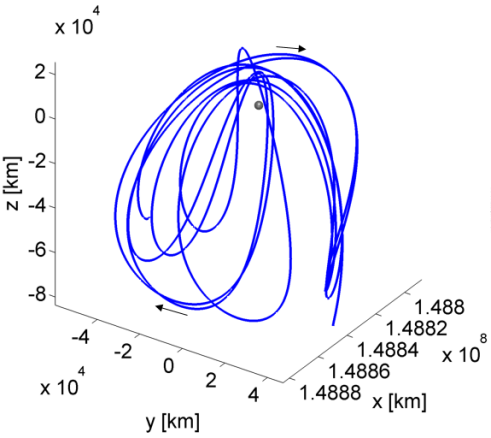

In the selenocentric reference system.

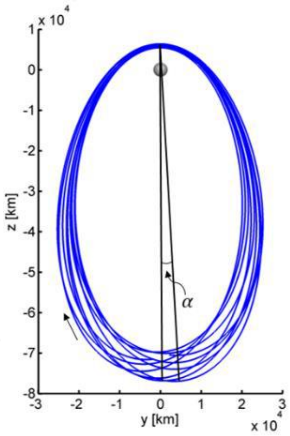

In the Earth-Moon rotating system seen from the Earth

Fig. 3-15 The Gateway's Near-Rectilinear Halo Orbit. The figure is taken from [25].

3.3.2 Calculation Approach and Results

In 2018, NASA published the Gateway's NRHO as a .bsp-file which can be implanted in STK and will be used for the following analyses. [26]

The following assumptions have been made for the scenario in STK to simulate the coverage:

- Communication between the Earth and the landing region can be achieved directly above the local horizon with an elevation angle of 0° above the horizon. This is possible because the Moon has no atmosphere allowing for unrestricted communication at low elevation angles.
- Communication can be achieved as soon as any line-of-sight with the Earth's surface can be attained. The simulation uses multiple facilities on the Earth's surface with coverage cones of 90° to simulate this.
- The scenario timeframe spans over one year from 30. Dec 2021 17:01:32.782 to 01. Jan 2023 22:12:23.081. This timeframe includes exactly 56 orbits of the Gateway, starting and stopping the scenario as the Gateway is located at its periapsis above the north pole.

These assumptions together with the same calculation approach used in 3.2.1 lead to the coverage results in Tab. 3-9.

Tab. 3-9 Coverage results via the Gateway for the potential landing regions. The mean values do not include the values determined for the Shackleton crater.

Landing Region	Coverage Time [%]	Maximum Gap Duration [h]	Average Gap Duration [h]	Average Number of Gaps/Year [-]
Mean value over all landing regions (excluding Shackleton)	97.56	3.97	3.81	56.69
001	97.58	3.96	3.82	56.69
004	97.57	3.98	3.83	56.69
007	97.57	4.01	3.84	56.69
011	97.57	3.97	3.84	56.69
102	97.69	3.83	3.65	56.69
105	97.52	4.12	3.92	56.69
Mount Kocher	97.61	3.95	3.78	56.69
Shackleton (for comparison)	97.43	4.22	4.06	56.69

The Gateway enables communication with the landing regions over 97% of the time. The average number of gaps per year shows that the communication gaps only occur once a week when the Gateway is close to its periapsis above the north pole. Unfortunately, the duration of the communication gaps spanning multiple hours is not well suited for human missions.

The coverage time averaged over the far side of the Moon is 54.50%. While the entire southern hemisphere has almost 100% coverage provided by the Gateway, the northern hemisphere of the far side can only communicate with the Earth when the Gateway is close to its periapsis. Due to its highly elliptical orbit this time span is proportionally small and therefore the coverage time between the Gateway and the north pole is only 1.12% (Fig. 3-16).

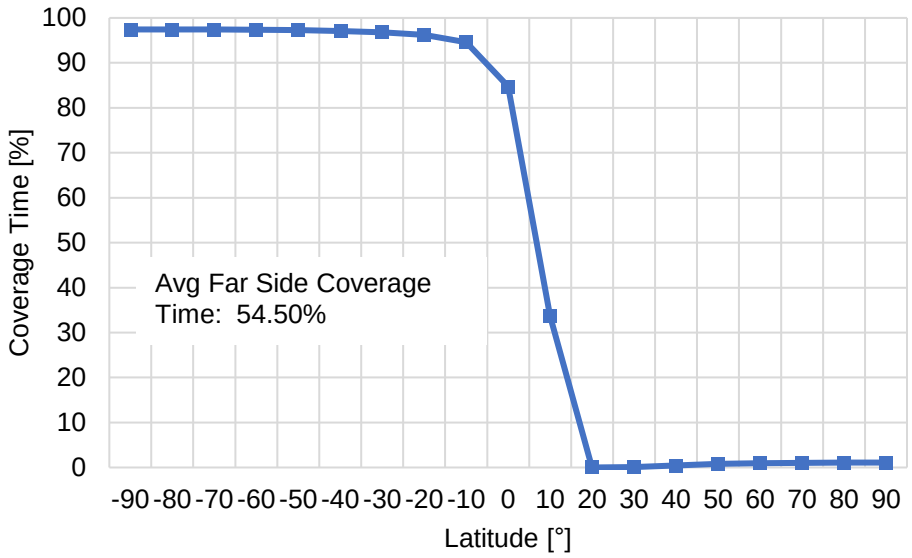

Fig. 3-16 Lunar far side coverage via Gateway.

These results match the results published by the Interagency Operations Advisory Group in 2019 in their “Lunar Communications Architecture” report. Fig. 3-17 is taken from this report and shows the maximum communication gaps between the lunar surface and the Gateway. Only considering the far side, the coverage minimum is also located at longitude 180° and latitude 20°. [27, p. 43]

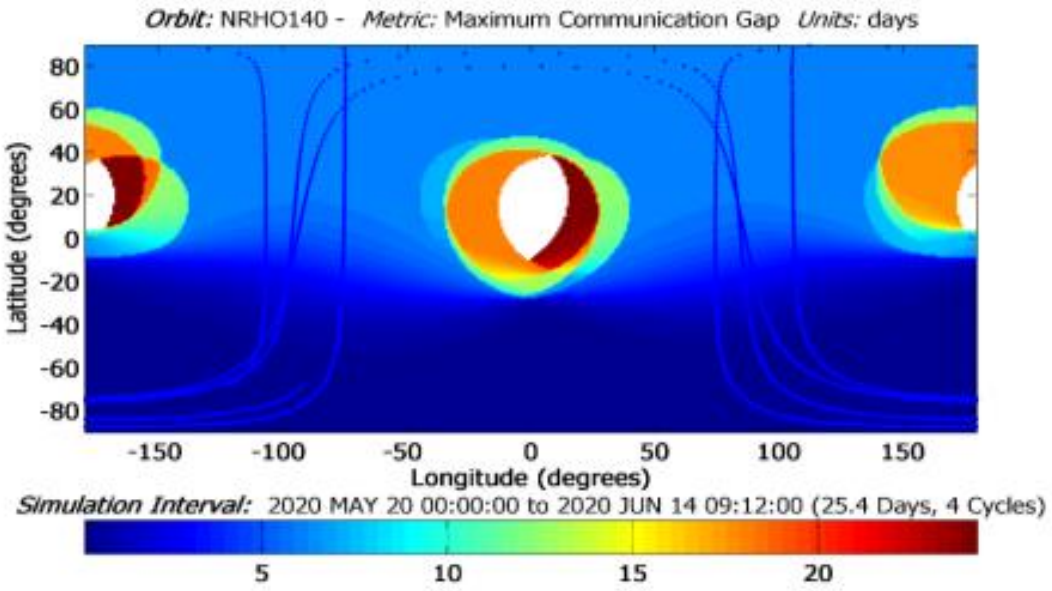

Fig. 3-17 Maximum Communication Gap between the lunar surface and the Gateway. The figure is taken from [27].

3.4 Communication via the Lunar Gateway and Complementary Satellites

3.4.1 Complementary Satellites on the Same Orbit as the Lunar Gateway

Using the Gateway as the only relay node between the landing sites and the Earth leads to communication gaps spanning multiple hours. To compensate for that, a second relay satellite could be placed on the same orbit as the Gateway with a phase shift in the mean anomaly of 180°. This means that one of the relay nodes would reach the apoapsis exactly when the other one reaches the periapsis, filling the communication gaps. The results can be seen in Tab. 3-10.

Tab. 3-10 Coverage results for the potential landing regions via the Gateway and an additional relay satellite on the same orbit with a mean anomaly phase shift of 180°. The mean values do not include the values determined for the Shackleton crater.

Landing Region	Coverage Time [%]	Maximum Gap Duration [h]	Average Gap Duration [h]	Average Number of Gaps/Year [-]
Mean value over all landing regions (excluding Shackleton)	100.00	0.00	0.00	0.00
001	100.00	0.00	0.00	0.00
004	100.00	0.00	0.00	0.00
007	100.00	0.00	0.00	0.00
011	100.00	0.00	0.00	0.00
102	100.00	0.00	0.00	0.00
105	100.00	0.00	0.00	0.00
Mount Kocher	100.00	0.00	0.00	0.00
Shackleton (for comparison)	100.00	0.00	0.00	0.00

While the second satellite in the NRHO enables a coverage time of 100% for all the potential landing regions, the placement of the spacecraft in this special orbit has disadvantages. The targeted NRHO exhibits almost stable characteristics, but an uncontrolled spacecraft will eventually fall into a different orbit closer to the Moon. The required delta-v for stationkeeping depends heavily on the spacecraft's shape, as solar pressure and gravity gradients affect the spacecraft's attitude and orbit [24, p. 1]. It was calculated that the Gateway would need around 2 m/s delta-v for stationkeeping per year, which will be provided by xenon engines [24, p. 7]. Using this unstable halo orbits limits the overall mission time possible for the satellite. This is because the satellite will not be visited by spacecrafts which can be bring new propellant like it is the case for the Gateway.

Fig. 3-18 shows the coverage of the lunar far side. The average far side coverage time only increased by 9% compared to the results with the Gateway alone. The north pole's coverage time is only 2.245%.

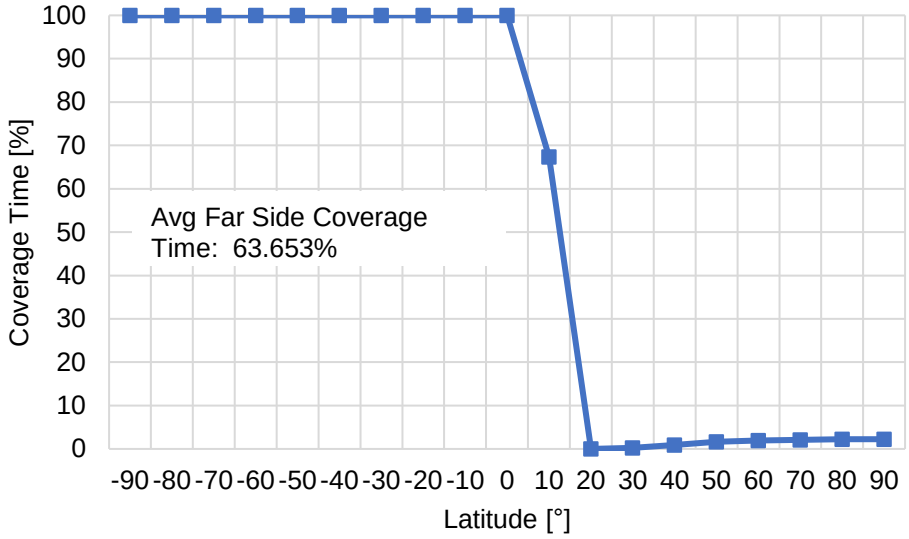

Fig. 3-18 Lunar far side coverage via Gateway and an additional relay satellite on the same orbit with a mean anomaly phase shift of 180°.

3.4.2 Complementary Satellites on a Different Orbit than the Lunar Gateway

3.4.2.1 Approach to Determine the Most Suitable Complementary Satellite

The previous chapter showed that it is possible to fully cover all the potential landing sites over the entire scenario timeframe with just one additional satellite to the Gateway. To find the most suitable satellite orbit, the MATLAB® script "STK_Constellation_Simulation.m" from chapter 3.2 simulated a total of 5409 different constellations with a runtime of 268.53 h, or about 11.19 days. The script placed the Gateway in its fixed orbit and the additional satellite was set in a variety of different orbits to find the one resulting in the highest score.

The script uses the same STK scenario assumptions as in 3.3.2.

- Communication between the Earth and the landing region can be achieved directly above the local horizon with an elevation angle of 0° above the horizon This is possible because the Moon has no atmosphere allowing for unrestricted communication at low elevation angles.
- Communication can be achieved as soon as any line-of-sight with the Earth's surface can be attained. The simulation uses multiple facilities on the Earth's surface with coverage cones of 90° to simulate this.
- The scenario timeframe spans over one year from 30. Dec 2021 17:01:32.782 to 01. Jan 2023 22:12:23.081. This timeframe includes exactly 56 orbits of the Gateway, starting and stopping the scenario as the Gateway is located at its periapsis above the north pole.

As the number of possible orbits around a celestial body is infinite, it is necessary to reduce the number of orbits drastically. The insertion of the additional satellite in STK

uses the six orbital elements necessary to define an orbit and simulates it in a two-body gravitational system. The script uses the following six orbital elements, previously shown in Fig. 3-7.

- apoapsis height
- periapsis height
- inclination
- longitude of the ascending node
- argument of periapsis
- true anomaly

As the satellite uses a two-body gravitational simulation, the Moon rotates underneath the satellite's orbital plane while the satellite's longitude of ascending node never changes. Since both, the Moon and the Earth rotate around their own axis, this should average the results. Therefore, over the entire scenario timeframe, the setting of the ascending node should not have any impact on the coverage results. This will be tested later with the final results.

It is assumed that the best possible result for south pole coverage can be achieved if the additional satellite is exactly over the south pole when the Gateway passes over the north pole. This must be true for every Gateway revolution. This means that the orbit period of the additional satellite must be an exact fraction of the Gateway's orbit period. Thus, every time the Gateway completes one full orbit, the additional satellite completes exactly 1, 2, 3 or more orbits. If a given periapsis is set, this limits the possible orbits drastically. There is only a finite number of possible apoapsis heights higher than the periapsis height that result in an exact fraction of the Gateway's orbit period. Fig. 3-19 shows all the 44 possible apoapsis heights for a periapsis height of 1000 km above the lunar surface. The orbit periods range from 1/1 to 1/44 of the time the Gateway needs to complete one rotation around the Moon.

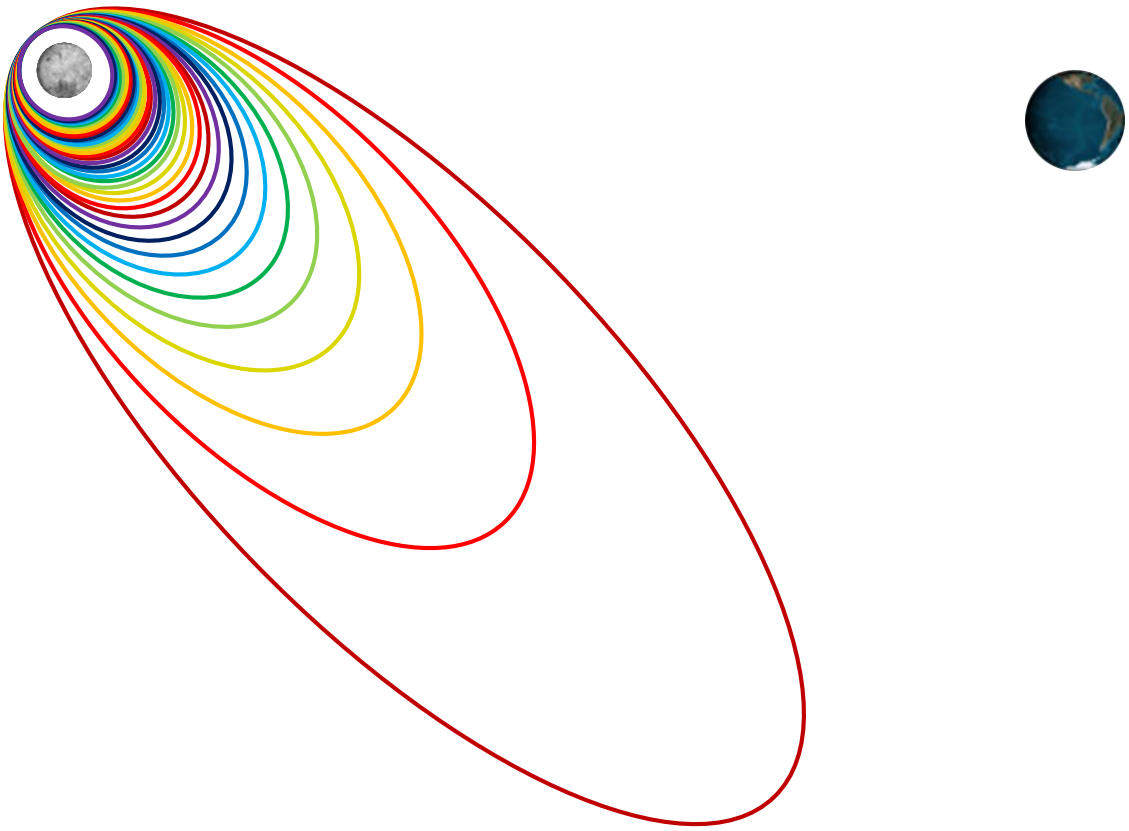

Fig. 3-19 The 44 possible apoapsis heights in synchronization with the Gateway's orbit period at a periapsis height of 1000 km.

To limit the possibilities further, it is assumed that the best coverage results can be achieved with an inclination of 90°, based on the results shown in Fig. 3-12 in chapter 3.2.3. This leaves the periapsis height and the argument of periapsis without any restrictions. To keep the simulation time reasonable, those two parameters are increased stepwise. The argument of periapsis is increased in 22.5° steps from 90° to 270° (Fig. 3-20). The true anomaly is also fixed to be exactly above the south pole when the Gateway is above the north pole.

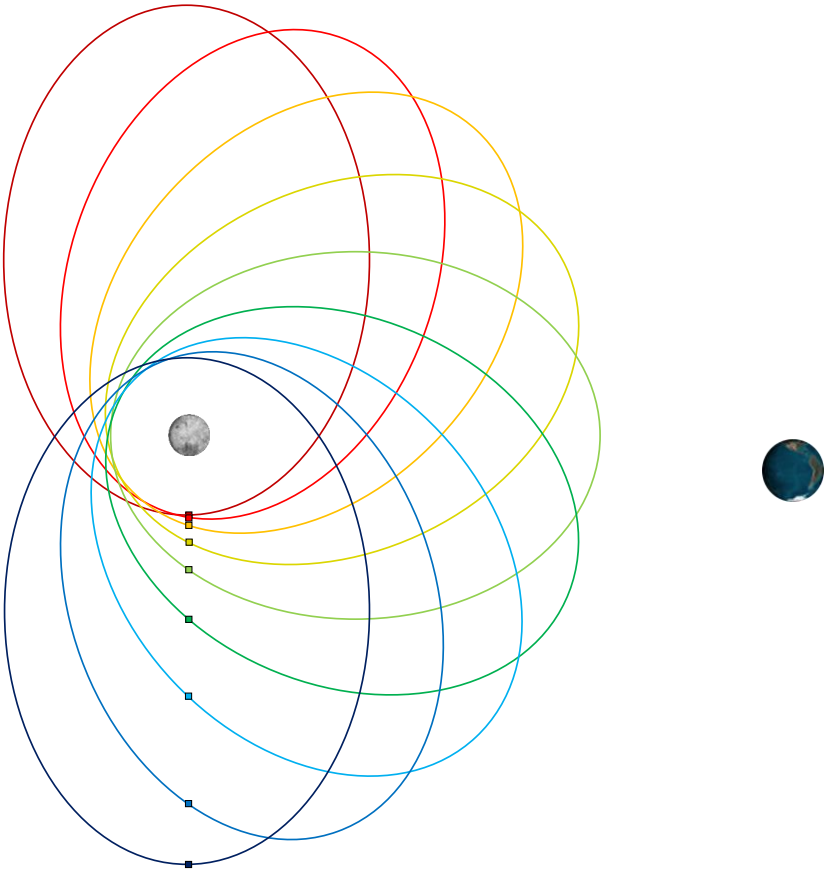

Fig. 3-20 Increase of the argument of periapsis in 22.5° steps from 90° to 270°.

The periapsis heights were set to be 50 km, 100 km, 200 km, 400 km, 500 km, 800 km, 1000 km, 1500 km, 2000 km, 3000 km, 5000 km, 8000 km, 10000 km, 15000 km, 20000 km and 25000 km. Larger periapsis heights would result in orbit periods greater than the Gateway's. Additionally, all the possible circular orbit heights that are synchronized with the Gateway's orbit period were calculated and simulated as well. This results in a total of 5109 possible orbits for the additional satellite.

As before, the measured values for each landing region and each constellation are:

- the coverage time [%],
- the maximum gap duration [h] during which no line-of-sight is present,
- the average gap duration [h],
- the average number of gaps per year [-],
- the average number of assets available [-],
- the coverage time of the north pole [%] and
- an approximation of the average far side coverage [%].

3.4.2.2 Results

The score system shown in 3.2.4 is used again to evaluate the different constellations and to find the most suitable one. The measured values selected for the score calculation are:

- the maximum gap duration [h] during which no line-of-sight is present,

- the coverage time of the north pole [%],
- the average far side coverage [%] and
- the maximum far side coverage [%] somewhere on the far side of the Moon between the latitudes -80° and 80°.

The following weightings and times were set to the same values as in 3.2.4 according to their importance (3-8) to (3-13).

$$t_{GapAllowed} = 600\ s \quad \textbf{(3-8)}$$

$$w_{Gap} = 1 \quad \textbf{(3-9)}$$

$$w_{Sha} = 0.5 \quad \textbf{(3-10)}$$

$$w_{NP} = 0.3 \quad \textbf{(3-11)}$$

$$w_{AFS} = 0.15 \quad \textbf{(3-12)}$$

$$w_{MFS} = 0.3 \quad \textbf{(3-13)}$$

Selecting the best scores for the first six different orbit periods results in the outcomes shown in Tab. 3-11. A general trend can be observed that a smaller orbit period leads to poorer results. The best results can be achieved with an orbit period that matches the Gateway's orbit period.

A more detailed table of the constellations with the best results can be seen in the appendix in Tab. 4-3.

Tab. 3-11 Results of the first approach to determine the best Satellites in addition to the Gateway

Orbit Period / Orbit Period Gateway [-]	Argument of Periapsis [°]	Apoapsis Height [km]	Periapsis Height [km]	Inclination [°]	Mean Coverage Time [%]	Mean Maximum Gap Duration [h]	Mean Average Gap Duration [h]	Mean Average Number of Gaps/Year [-]	North Pole Coverage Time [%]	Average Far Side Coverage [%]	Maximum Far Side Coverage [%]	Score [-]
1	270	49856.13	15000	90	100	0	0	0	80.75	86.80	100	96.6
1/2	270	24570.99	15000	90	100	0	0	0	62.65	80.61	100	93.7
1/3	90	14687.64	14687.64	90	100	0	0	0	47.75	75.69	100	91.4
1/4	90	11821.17	11821.17	90	100	0	0	0	47.00	75.02	100	91.3
1/5	90	11894.05	8000	90	100	0	0	0	35.84	71.34	100	89.5
1/6	90	12219.46	5000	90	100	0	0	0	24.29	67.36	100	87.7

In addition to the Gateway, all the orbits shown in Tab. 3-11 achieve better results in north pole and far side coverage than a second satellite on the same orbit as the Gateway. The best score is achieved by a high polar orbit with the same orbit period as the Gateway, an opposing argument of periapsis, and a smaller eccentricity than the Gateway. This constellation leads to a 100% coverage of all potential landing regions (Tab. 3-13).

To further optimize the result, the script decreases the step size between the periapsis heights while keeping all other orbital elements at their optimum. The apoapsis height is adjusted accordingly to achieve the same orbit period as the Gateway. Previously, the highest score was found at 15000 km so the optimum must be between the steps of 10000 km and 20000 km. Decreasing the step size to 100 km showed that the optimum had to lie between 10500 km and 10700 km. The last iteration decreased the step size to 1 km and the periapsis height which achieves the overall highest score of 97.646 is found at 10527 km (Tab. 3-12). The additional satellite and the Gateway are shown in Fig. 3-21 as well as their coverage results in Tab. 3-13.

A more detailed table of the constellations with the best results can be seen in the appendix in Tab. 4-4.

Tab. 3-12 Results for the best Satellites in addition to the Gateway. The best additional Satellite is positioned at a Periapsis Height of 10527 km.

Orbit Period / Orbit Period Gateway [-]	Argument of Periapsis [°]	Apoapsis Height [km]	Periapsis Height [km]	Inclination [°]	Mean Coverage Time [%]	Mean Maximum Gap Duration [h]	Mean Average Gap Duration [h]	Mean Average Number of Gaps/Year [-]	North Pole Coverage Time [%]	Average Far Side Coverage [%]	Maximum Far Side Coverage [%]	Score [-]
1	270	57329.13	10527	90	100	0	0	0	87.71	89.30	99.99	97.6
1	270	54328.13	10528	90	100	0	0	0	87.70	89.30	99.99	97.6
1	270	54327.13	10529	90	100	0	0	0	87.70	89.30	99.99	97.6
1	270	54.256.13	10600	90	100	0	0	0	87.60	89.23	99.99	97.6
1	270	54156.13	10700	90	100	0	0	0	87.45	89.20	99.99	97.6
1	270	49856.13	15000	90	100	0	0	0	80.75	86.80	100	96.6

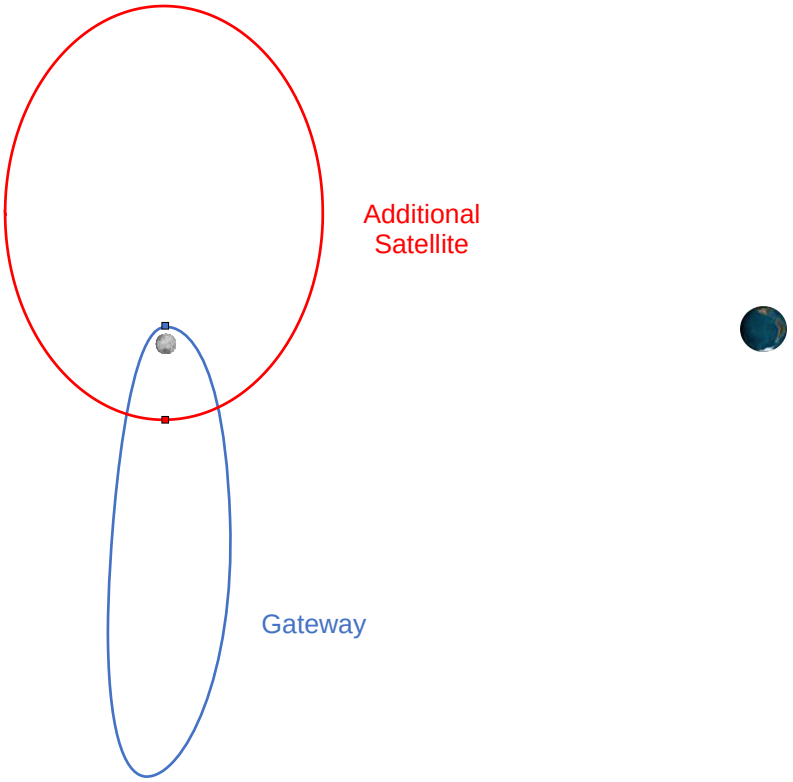

Fig. 3-21 The best coverage results are achieved by an additional satellite with a high polar orbit with the same orbit period as the Gateway, an opposing argument of periapsis, an apoapsis height of 54329.13 km and a periapsis height of 10527 km.

Tab. 3-13 Coverage results of all potential landing sites using the constellation shown in Fig. 3-21.

Landing Region	Coverage Time [%]	Maximum Gap Duration [h]	Average Gap Duration [h]	Average Number of Gaps/Year [-]
Mean value over all landing regions (excluding Shackleton)	100.00	0.00	0.00	0.00
001	100.00	0.00	0.00	0.00
004	100.00	0.00	0.00	0.00
007	100.00	0.00	0.00	0.00
011	100.00	0.00	0.00	0.00
102	100.00	0.00	0.00	0.00
105	100.00	0.00	0.00	0.00
Mount Kocher	100.00	0.00	0.00	0.00
Shackleton (for comparison)	100.00	0.00	0.00	0.00

To prove the stability of the results, multiple weighting combinations were tested to evaluate whether the scores change significantly enough for other orbits to reach a higher score than the orbit shown in Fig. 3-12 with a Periapsis Height of 10527 km. The following combinations were tested and each one lead to the same order as shown before:

$w_{Gap} = 1$	$w_{Gap} = 1$	$w_{Gap} = 1$	$w_{Gap} = 1$	$w_{Gap} = 1$
$w_{Sha} = 1$	$w_{Sha} = 1$	$w_{Sha} = 0.1$	$w_{Sha} = 0.1$	$w_{Sha} = 0.1$
$w_{NP} = 1$	$w_{NP} = 0.1$	$w_{NP} = 1$	$w_{NP} = 0.1$	$w_{NP} = 0.1$
$w_{AFS} = 1$	$w_{AFS} = 0.1$	$w_{AFS} = 0.1$	$w_{AFS} = 1$	$w_{AFS} = 0.1$
$w_{MFS} = 1$	$w_{MFS} = 0.1$	$w_{MFS} = 0.1$	$w_{MFS} = 0.1$	$w_{MFS} = 1$

Setting multiple values to 0 would lead to an excess of constellations reaching a score of 100. Therefore, the minimum weighting was set to 0.1. Since each of these combinations lead to the same results, it can be concluded that the results are indeed stable.

At the beginning of the analysis, the assumption was made that the ascending node of the inserted non-halo orbit does not influence the coverage results. To prove this assumption, the orbits with the highest score shown in Tab. 3-11 were inserted again in STK with varying ascending nodes. Fig. 3-22 shows all the calculated values of each orbit and Gateway combination over the varying ascending node of the inserted satellite. As all lines are almost completely horizontal, the calculations demonstrate that the assumption was right and that the longitude of the ascending node of the additional satellite does not influence the coverage results.

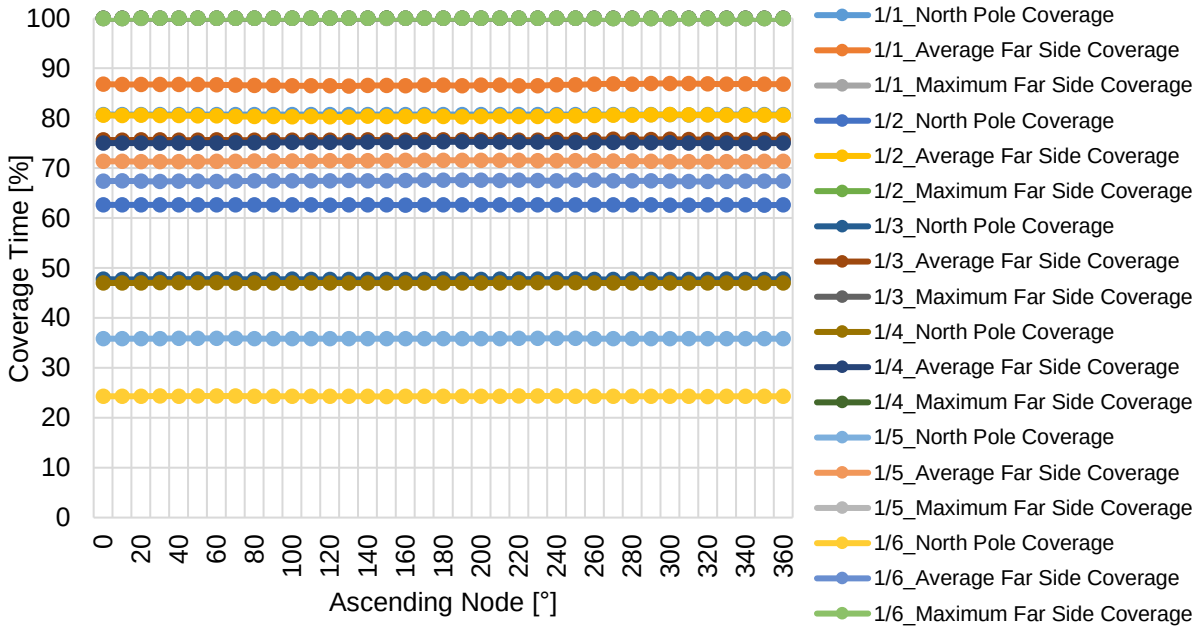

Fig. 3-22 Measured values of the selected orbits in Tab. 3-11 over varying the ascending node in 10° steps. The fractions shown in the variables' names refer to the orbital period in ratio to the Gateway's orbital period.

4 Discussion

4.1 Assumptions

During the course of this paper, multiple assumptions and simplifications were made. The lunar precession was neglected in the simulations to allow for reasonable computing times. The precession affects how the Moon is tilted towards the Earth. This could have a relatively big impact on the coverage time using direct communication without relay satellites because the line of sight between the lunar south pole and the Earth is constantly only a few degrees above the horizon. The coverage with relay satellites would be less impacted by this since the line of sight between the landing site and the current asset of the relay constellation is higher above the horizon most of the time. It can be assumed that the axial precession has the biggest impact on the total tilt angle between the Moon and the Earth. The maximum difference between two positions would therefore be about two times the 1.54° lunar obliquity to ecliptic (Fig. 3-2). The constellation determined in 3.4.2.2, which consists of the Gateway and one additional satellite, has a 100% coverage inside the Shackleton crater. The mean elevation angle of the surrounding topography in the middle of the Shackleton crater is 20.80°, which is significantly more than for the potential landing spots and the possible tilt angle due to the lunar precession. Therefore, it can be concluded that the lunar precession has no impact on the coverage of the final relay constellation determined in 3.4.2.2.

Another simplification was the neglection of orbit stability and the need for active station keeping which would have a big impact on the final selection of the relay satellite constellation. Stable orbits allow for longer and cheaper operation. The cost benefit of stable orbits might make the usage of two lower satellites more favorable than the usage of one satellite in a high orbit.

4.2 Accuracy Analysis of the Coverage Simulations

To analyze the accuracy of the “STK_Constellation_Simulation.m” MATLAB® script, a plausibility check is employed using the data provided by NASA for the Gateway’s NRHO as well as a comparison to the Gateway’s NRHO coverage with results in other literature. The simulation uses a SPICE-Propagator file published by NASA to simulate the Gateway’s NRHO [26]. The orbit is described as a “15 year near-continuous phased reference of an L2 southern family Near Rectilinear Halo Orbit (NRHO) with a 9:2 lunar synodic resonance, wherein there are 9 revolutions for every 2 lunar synodic periods” [26]. A lunar synodic period spans over 29.53 days [20]. With a 9:2 lunar synodic resonance, the Gateway therefore has an orbit period of 6.56 days around the Moon. The connection between the south pole and Gateway is lost once per orbit when it passes through its periapsis above the north pole. In the simulation time of 367.216 days, a total of 57 gaps were detected. Since the simulation both started and ended as the Gateway was positioned at its periapsis, one additional gap was detected. A rate of 56 gaps in 367.216 days results in a gap every 6.557 days. Therefore, it can be assumed that the simulation detected all the connections between the south pole and the Gateway correctly.

For further analysis of the simulation’s accuracy, a comparison to other literature is carried out. In 2019 the Interagency Operations Advisory Group published “The Future

Lunar Communications Architecture" report [27]. It included the global lunar coverage provided the Gateway's NRHO (Fig. 4-1).

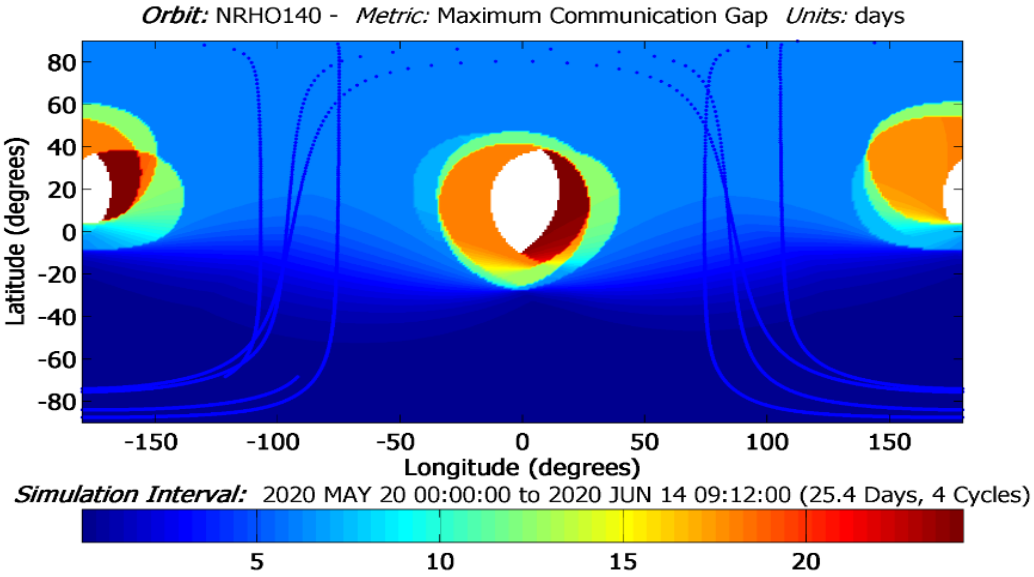

Fig. 4-1 Maximum Communication Gap between the lunar surface and the Gateway. The figure is taken from [27]

It shows the coverage of the far side of the Moon at the very right and left of the graph at -180° and 180°, both representing the same longitude. A coverage minimum of 0% can be seen at 20° latitude. A coverage of almost 100% is depicted beneath -10° latitude, and above 40° latitude, a slight improvement can be seen towards the north pole.

Fig. 4-2 shows the coverage results at 180° longitude calculated by the "STK_Constellation_Simulation.m" MATLAB® script. The same trends can be observed. It can be concluded that the script simulates and calculates the coverage between the lunar surface and a satellite correctly.

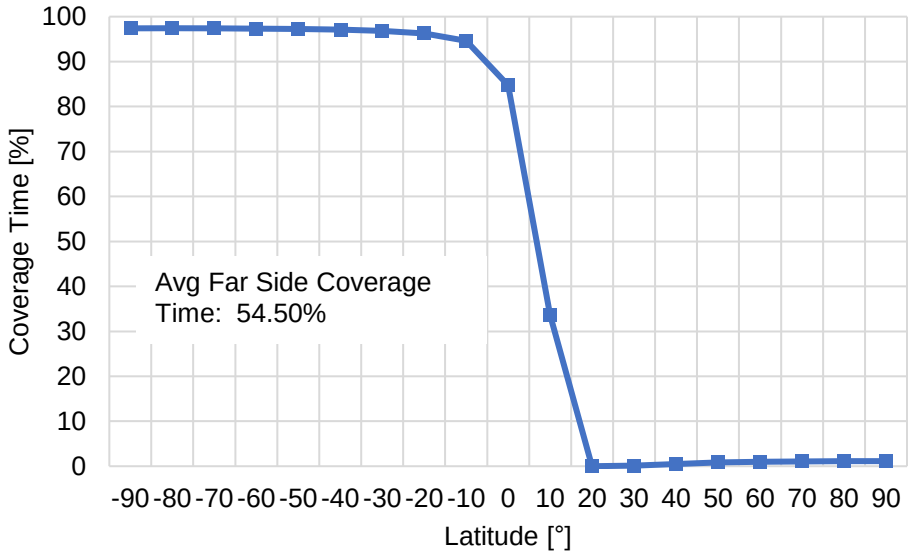

Fig. 4-2 Lunar far side coverage at 180° longitude via Gateway. The values were simulated and calculated by the "STK_Constellation_Simulation.m" MATLAB® script.

4.3 Deviation Analysis of the Azimuth Elevation Masks

To maximize the stability of the results, a deviation analysis of the outputs of the "Local_Horizon.m" MATLAB® script is performed. In the paper "Lunar Pole Illumination and Communication Statistics Computed from GSSR Elevation Data" by Scott Bryant released in 2010 by the California Institute of Technology and the Jet Propulsions Laboratory, an azimuth elevation mask of the lunar surface is implemented [16, p. 8]. Recreating the same local horizon from the same viewpoint with the same parameters using the MATLAB® script written within the scope of this paper, leads to the deviations shown in Fig. 4-3. The green line was plotted by the "Local_Horizon.m" MATLAB® script and is placed over the graph from the aforementioned literature. The maximum deviation is 1.79° at the 62° azimuth angle.

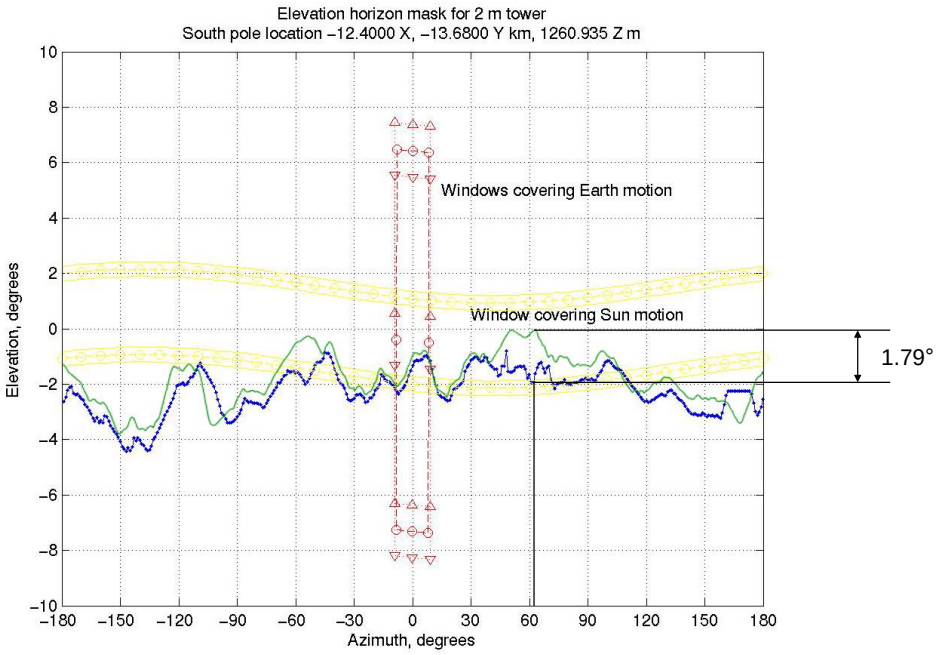

Fig. 4-3 Deviation between the local horizon computed by the MATLAB® script "Local_Horizon.m" (green line) and a graph presented in the literature (blue line). The green line and the deviation was added to the graph taken from [16].

This deviation could result from the fact that the script uses straight lines upon the lunar stereographic map data as line-of-sights. Straight lines on a sphere, so called orthodromes, are not represented by straight lines on stereographic maps, except for orthodromes passing through the poles. The further the viewpoint is located away from the map's center, in this case the south pole, the greater the apparent curvature gets. The highest curvature can be observed with a line-of-sight to east or west. Fig. 4-3 shows the deviation between a straight line on a stereographic projection and an actual straight orthodrome on the spherical surface at a viewpoint on the -80° latitude and a line-of-sight to east and west, resulting in the maximum deviation possible at this latitude. As all potential landing sites used for the calculations in this paper have a latitude closer to the south pole, the deviation shown in Fig. 4-4 is greater than any experienced in this paper. The maximum deviation for this example, on a sphere the size of the Moon, at a maximum viewing distance of 200 km is 0.995 km which correlates to an azimuth deviation of only 0.286° (Fig. 4-5). Therefore, it can be

assumed that the deviations appearing in the graphs are not a result of the usage of straight lines as lines-of-sight on the stereographic map data.

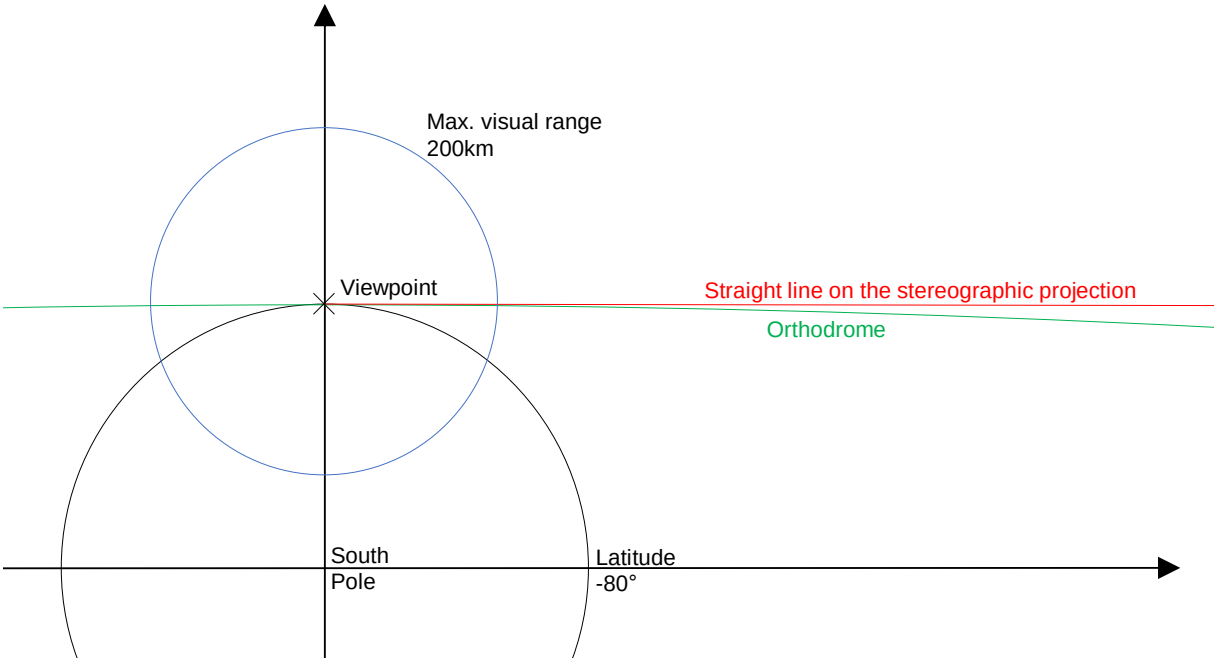

Fig. 4-4 Apparent curvature of a straight orthodrome on a stereographic projection passing through a minimal latitude of -80°. All relative sizes are true to scale.

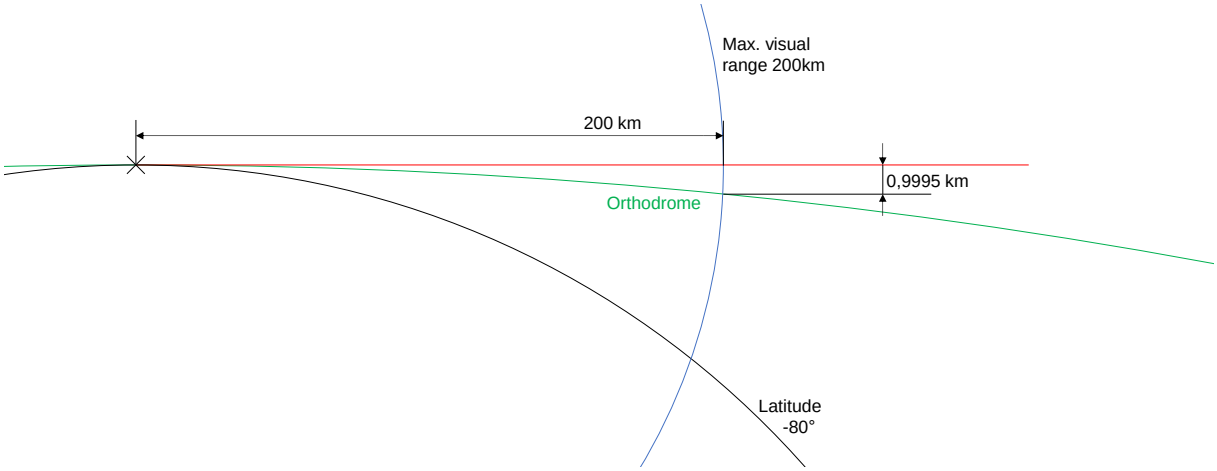

Fig. 4-5 Close-up of Fig. 4-4 with an increased orthodrome curvature for better illustration.

It is not clear what causes the deviations. They could be a result of different elevation data used or possibly small errors in the script. No further simplifications other than the usage of straight lines as line-of-sights are used by the script.

To demonstrate the independence of the constellation result from the deviation in the AzEl-Masks, the coverage of the landing sites was calculated again in STK. This time, all AzEl-Masks were increased for all azimuth angles by the deviation of 1.79° shown in Fig. 4-3. This simulates a higher horizon for every landing site. Tab. 4-1 shows the coverage results of all the landing regions and the Shackleton crater for the constellation with the highest score in Tab. 3-11. The table shows that the result is

independent from the deviation caused by the “Local_Horizon.m” MATLAB® script as the coverage is still 100% for all landing regions.

Tab. 4-1 Coverage results of the constellation with the overall highest score shown in Fig. 3-21 after increasing all azimuth elevation masks by the maximum deviation occurring in the comparison to a local horizon found in other literature (Fig. 4-3).

Landing Region	Coverage Time [%]	Maximum Gap Duration [h]	Average Gap Duration [h]	Average Number of Gaps/Year [-]
Mean value over all landing regions (excluding Shackleton)	100.00	0.00	0.00	0.00
001	100.00	0.00	0.00	0.00
004	100.00	0.00	0.00	0.00
007	100.00	0.00	0.00	0.00
011	100.00	0.00	0.00	0.00
102	100.00	0.00	0.00	0.00
105	100.00	0.00	0.00	0.00
Mount Kocher	100.00	0.00	0.00	0.00
Shackleton (for comparison)	100.00	0.00	0.00	0.00

A further analysis in STK is made to determine the maximum horizon height for a landing spot near the south pole using this constellation. By increasing the elevation angle of a flat horizon directly at the south pole and measuring the resulting coverage, the quality of coverage that can be expected in more difficult terrain near the south pole with high AzEl-Masks is demonstrated. Fig. 4-6 and Tab. 4-2 show the coverage time [%] and maximum communication gap durations [h] for sites at the south pole with increasing elevation angles. In this simulation, the elevation angles remain constant along the azimuth angles and the AzEl-Masks are therefore shaped like simple circular cones.

Up to an elevation angle of 15°, this constellation achieves a coverage of 100%. The higher the elevation angle gets, the further the coverage time decreases, and the communication gap duration increases. At an elevation angle of 50° the constellation still achieves 96.29% coverage time.

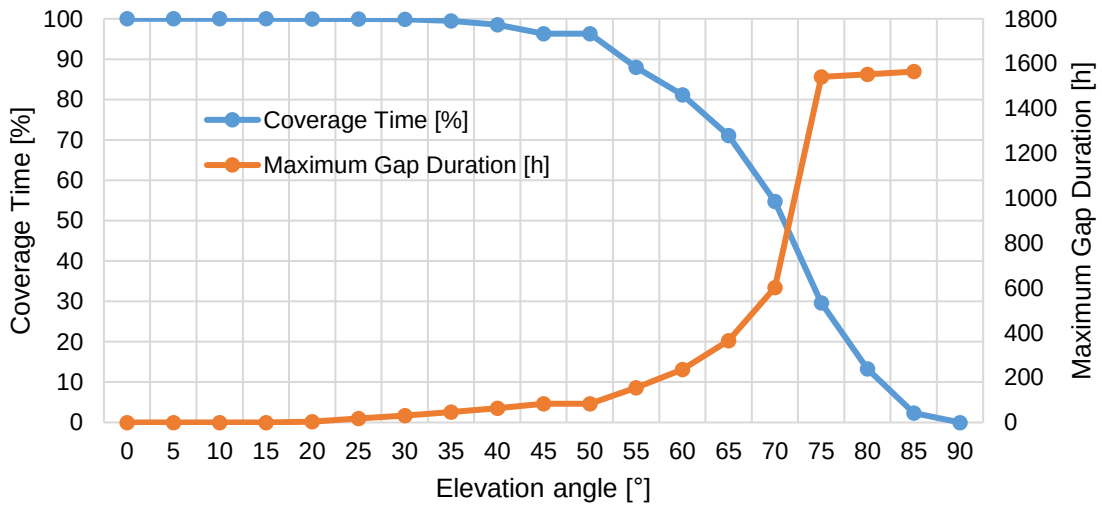

Fig. 4-6 Coverage time and communication gap duration for increasing elevation angles at a site positioned directly at the south pole.

Tab. 4-2 Coverage time and communication gap duration for increasing elevation angles at a site positioned directly at the south pole.

Constant Elevation Angle of the Local Horizon at the South Pole [°]	Coverage Time [%]	Maximum Gap Duration [h]
0	100.00	0.00
5	100.00	0.00
10	100.00	0.00
15	100.00	0.00
20	100.00	3.50
25	99.98	17.21
30	99.88	31.40
35	99.51	46.60
40	98.55	63.52
45	96.29	83.20
50	96.29	83.20
55	87.95	154.28
60	81.14	236.15
65	71.07	365.12
70	54.76	602.22
75	29.64	1541.48
80	13.30	1552.82
85	2.36	1564.49
90	0.00	-

4.4 Future Work

All the MATLAB® scripts written within the scope of this paper were created in such a way so as that they can be easily used or modified for other similar analyses in future work. The “Local_Horizon.m” script can be used with any .jp2 type DEM-data in stereographic projection of any size. It can therefore be used for analyses on any celestial body. DEM-data of the north pole would have to be used as though it was mirrored onto the south pole because the script’s allowed coordinates only reach from 0° to -90° latitude. The “STK_Direct_Contact_Simulation” can be used for any points on the surface of any celestial body supported by STK. The landing sites’ coordinates and their associated celestial body can easily be modified to any point. The “STK_Constellation_Simulation” script’s input parameter can be set for multiple applications. It can place walker constellations with up to 20 satellites in any orbit configuration as seen in 3.2. Furthermore, it can place one satellite in all possible orbit period resonances as seen in 3.4. With small modifications, the script can be used around any celestial body supported by STK.

To fully verify the results of this work, further analyses of the impact of lunar precession and the orbit stability of the calculated orbits would be necessary. Especially the cost aspect of station keeping due to orbit instability can have a big impact on the orbit selection.

4.5 Conclusion

The lunar south pole provides locations where a 100% communication coverage between the lunar surface and the Earth is directly possible. Both the Malapert and the Leibnitz Massif have shown to achieve full coverage. These locations could be used for the early phases of the upcoming lunar exploration while relay satellites and the Gateway are not yet placed in orbit. Relay satellites allow for a more flexible selection of the landing site and even provide coverage at sites with a high local horizon.

The Gateway alone achieves a south pole coverage of over 97%, an average far side coverage of 54.50%, a maximum far side coverage of over 97.43%, but only a 1.12% coverage time at the north pole. The communication gap to the south pole of over 3 h does not make it capable of providing an adequate coverage for human missions. By using elliptical orbits, the minimal number of relay satellites needed for a 100% coverage of the south pole is two. As the Gateway’s highly elliptical orbit with an apoapsis above the south pole is very useful in such a relay constellation, the MATLAB® script “STK_Constellation_Simulation.m”, written within the scope of this paper, simulated 5409 different additional satellites to the Gateway to determine the best constellation including the Gateway as one of the relay nodes. The best additional satellite was then determined by the introduction of a score system and the results were successfully tested for their stability.

The best coverage results can be achieved by placing the additional satellite on an orbit with the same orbit period but a smaller eccentricity than the Gateway and an argument of periapsis opposing the Gateway’s argument of periapsis. The additional satellite with the best overall score had the following orbital elements:

- Apoapsis height: 54329.13059 km
- Periapsis height: 10527 km
- Inclination: 90°

- Longitude of the ascending node: not important
- Argument of periapsis: 270°
- True anomaly: set to be above the south pole as the Gateway reaches its periapsis above the north pole

The constellation, which uses the Gateway and this additional satellite, results in a coverage of 100.00% for all potential landing regions while also providing:

- 87.71% coverage at the north pole,
- 99.99% coverage on a point on the far side of the Moon between -80° an 80° latitude,
- 89.30% average far side coverage and
- 100.00% coverage at the middle of the Shackleton crater.

These results show that the communication needed for all the planned missions to the lunar surface can be achieved by launching just one additional satellite into lunar orbit.

A References

[1] N. R. Council, Sciences, Division on Engineering and Physical, S. S. Board, and Moon, Committee on the Scientific Context for Exploration of the, *The scientific context for exploration of the moon*. Washington, D.C.: National Academies Press, 2007.

[2] H. Falcke, “Riding Big Waves: The last frontier in astronomy - radio observations on the moon,”

[3] C. M. Pieters *et al.,* “Character and spatial distribution of OH/H2O on the surface of the Moon seen by M3 on Chandrayaan-1,” *Science (New York, N.Y.)*, vol. 326, no. 5952, pp. 568–572, 2009, doi: 10.1126/science.1178658.

[4] A. R. Vasavada, D. A. Paige, and S. E. Wood, “Near-Surface Temperatures on Mercury and the Moon and the Stability of Polar Ice Deposits,” *Icarus*, vol. 141, no. 2, pp. 179–193, 1999, doi: 10.1006/icar.1999.6175.

[5] P. Gläser *et al.,* “Illumination conditions at the lunar south pole using high resolution Digital Terrain Models from LOLA,” *Icarus*, vol. 243, pp. 78–90, 2014, doi: 10.1016/j.icarus.2014.08.013.

[6] S. Li *et al.,* “Direct evidence of surface exposed water ice in the lunar polar regions,” *Proc Natl Acad Sci USA*, vol. 115, no. 36, pp. 8907–8912, 2018, doi: 10.1073/pnas.1802345115.

[7] NASA, “The Artemis Plan,” [Online]. Available: https://www.nasa.gov/sites/default/files/atoms/files/artemis_plan-20200921.pdf

[8] J. Crusan, “Gateway Update: NASA ADVISORY COUNCIL - Human Exploration and Operations Committee,” 2018.

[9] K. M. Coderre *et al.,* “Concept of Operations for the Gateway,” in *15th International Conference on Space Operations (SpaceOps 2018): Marseille, France, 28 May-1 June 2018*, Marseille, France, 2018.

[10] Cremins, Tom (HQ-AH000), “NASA’s Plan for Sustained Lunar Exploration and Development,” 2020.

[11] D. Kaschubek, M. Killian, and L. Grill, “System analysis of a moon base at the south pole: Considering landing sites, ECLSS and ISRU,” *Acta Astronautica*, 2021, doi: 10.1016/j.actaastro.2021.05.004.

[12] J. Stopar and H. Meyer, *Topographic Map of the Moon’s South Pole (80°S to Pole), Lunar and Planetary Institute Regional Planetary Image Facility, LPI Contribution 2169.* [Online]. Available: https://repository.hou.usra.edu/handle/20.500.11753/1254

[13] B. Pillot, M. Muselli, P. Poggi, P. Haurant, and J. B. Dias, “Development and validation of a new efficient SRTM DEM-based horizon model combined with optimization and error prediction methods,” *Solar Energy*, vol. 129, pp. 101–115, 2016, doi: 10.1016/j.solener.2016.01.058.

[14] G. Chin *et al.,* “Lunar Reconnaissance Orbiter Overview: The Instrument Suite and Mission,” (in En;en), *Space Sci Rev*, vol. 129, no. 4, pp. 391–419, 2007, doi: 10.1007/s11214-007-9153-y.

[15] The Planetary Data System, *ldem_75s_30m.jp2.* [Online]. Available: https://pds-geosciences.wustl.edu/lro/lro-l-lola-3-rdr-v1/lrolol_1xxx/data/lola_gdr/polar/jp2/

[16] S. Bryant, “Lunar Pole Illumination and Communications Statistics Computed from GSSR Elevation Data,” in *SpaceOps 2010 Conference*, Huntsville, Alabama, 04252010.

[17] C. Alexander, *The Endurance: Shackleton's legendary Antarctic expedition*. London: Bloomsbury, 1998.

[18] M. M. Nazeer, “Solar, Lunar and Venus Roles in Some Global Climatic Events,” *OALib*, vol. 07, no. 09, pp. 1–28, 2020, doi: 10.4236/oalib.1106419.

[19] D. A. Kring, J. E. Greuner, and D. B. Eppler, “Artemis III EVA Opportunities on Malapert and Leibnitz β Massifs,”

[20] D. R. Williams, *Moon Fact Sheet.* [Online]. Available: https://nssdc.gsfc.nasa.gov/planetary/factsheet/moonfact.html

[21] Wikimedia Commons contributors, *Lunar Orbit and Orientation with respect to the Ecliptic.* [Online]. Available: https://commons.wikimedia.org/w/index.php?title=File:Lunar_Orbit_and_Orientation_with_respect_to_the_Ecliptic.svg&oldid=561675270 (accessed: May 19 2021).

[22] A. Genova, B. Kaplinger, M. Wilde, and B. Aldrin, “Establishment and design of an earth-moon communications network in lunar polar orbit,” in *2018 IEEE Aerospace Conference: 3-10 March 2018*, Big Sky, MT, 2018, pp. 1–9.

[23] L. Snyder, *Orbital Elements.* [Online]. Available: https://en.wikipedia.org/w/index.php?title=File:Orbit1.svg#filelinks (accessed: Jun. 8 2021).

[24] C. P. Newman, D. C. Davis, R. J. Whitley, J. R. Guinn, and M. S. Ryne, “Stationkeeping, Orbit Determination, and Attitude Control for Spacecraft in Near Rectilinear Halo Orbits: Document ID: 20180006800,” [Online]. Available: https://core.ac.uk/download/pdf/161998349.pdf

[25] Du Chongrui, V. V. Koryanov, and C. Danhe, “Analysis of Orbital Movement Lunar Orbital Station,” *IOP Conf. Ser.: Mater. Sci. Eng.*, vol. 630, no. 1, p. 12027, 2019, doi: 10.1088/1757-899X/630/1/012027.

[26] NASA, *Deep Space Gateway.* [Online]. Available: https://naif.jpl.nasa.gov/pub/naif/misc/MORE_PROJECTS/DSG/

[27] Interagency Operations Advisory and Group Lunar Communications Architecture Working Group, “The Future Lunar Communications Architecture,” 2019.

B Appendix

Tab. 4-3 Best scores achieved at the first iteration of periapsis heights. The constellations consist of the Gateway and one additional satellite. The yellow-colored satellites scored the highest with respect to their orbit period.

Nr.	Longitude of Ascending Node [°]	Argument of Periapsis [°]	Apoapsis Height [km]	Periapsis Height [mkm]	Inclination [°]	OrbitPeriod / OrbitPeriod Gateway	Average Coverage Time [%]	Average Maximum Gap Duration [h]	Average Number of Assets Available [-]	Shackleton Coverage Time [%]	North Pole Coverage Time [%]	Average Far Side Coverage [%]	Maximum Far Side Coverage [%]	Score
5018	0	270	49856.13059	15000	90	1	100.00	0	1.16	100.00	80.75	86.80	100.00	96.55
4460	0	247.5	49856.13059	15000	90	1	100.00	0	1.18	100.00	79.06	86.38	100.00	96.30
3902	0	225	49856.13059	15000	90	1	100.00	0	1.24	100.00	73.54	84.51	100.00	95.44
5020	0	270	44856.13059	20000	90	1	100.00	0	1.25	100.00	72.23	83.97	100.00	95.23
4462	0	247.5	44856.13059	20000	90	1	100.00	0	1.26	100.00	70.78	83.76	100.00	95.02
3904	0	225	44856.13059	20000	90	1	100.00	0	1.31	100.00	66.27	82.40	100.00	94.33
3344	0	202.5	49856.13059	15000	90	1	100.00	0	1.34	100.00	63.33	81.51	100.00	93.88
5021	0	270	39856.13059	25000	90	1	100.00	0	1.34	100.00	63.24	81.21	100.00	93.85
4463	0	247.5	39856.13059	25000	90	1	100.00	0	1.35	100.00	62.25	81.02	100.00	93.70
5019	0	270	24570.9889	15000	90	0.5	100.00	0	1.32	100.00	62.65	80.61	100.00	93.73
4461	0	247.5	24570.9889	15000	90	0.5	100.00	0	1.33	100.00	61.64	80.45	100.00	93.58
3905	0	225	39856.13059	25000	90	1	100.00	0	1.38	100.00	59.35	80.24	100.00	93.26
3346	0	202.5	44856.13059	20000	90	1	100.00	0	1.38	100.00	58.81	80.29	100.00	93.19
3903	0	225	24570.9889	15000	90	0.5	100.00	0	1.36	100.00	58.66	79.65	100.00	93.13
3347	0	202.5	39856.13059	25000	90	1	100.00	0	1.42	100.00	54.86	78.96	100.00	92.58
3345	0	202.5	24570.9889	15000	90	0.5	100.00	0	1.41	100.00	54.04	78.37	100.00	92.43
2786	0	180	49856.13059	15000	90	1	100.00	0	1.48	100.00	49.27	77.83	100.00	91.76
2788	0	180	44856.13059	20000	90	1	100.00	0	1.48	100.00	49.39	77.67	100.00	91.76
2789	0	180	39856.13059	25000	90	1	100.00	0	1.48	100.00	49.45	77.45	100.00	91.76
558	0	90	32428.0653	32428.0653	90	1	100.00	0	1.48	100.00	49.51	77.03	100.00	91.74
2790	0	180	32428.0653	32428.0653	90	1	100.00	0	1.48	100.00	49.51	77.03	100.00	91.74
5022	0	270	32428.0653	32428.0653	90	1	100.00	0	1.48	100.00	49.51	77.03	100.00	91.74
5023	0	90	32428.0653	32428.0653	90	1	100.00	0	1.48	100.00	49.51	77.03	100.00	91.74
1116	0	112.5	32428.0653	32428.0653	90	1	100.00	0	1.48	100.00	49.51	77.03	100.00	91.74
3348	0	202.5	32428.0653	32428.0653	90	1	100.00	0	1.48	100.00	49.51	77.03	100.00	91.74
4464	0	247.5	32428.0653	32428.0653	90	1	100.00	0	1.48	100.00	49.51	77.03	100.00	91.74
3906	0	225	32428.0653	32428.0653	90	1	100.00	0	1.48	100.00	49.51	77.03	100.00	91.74
1674	0	135	32428.0653	32428.0653	90	1	100.00	0	1.48	100.00	49.51	77.03	100.00	91.74
2232	0	157.5	32428.0653	32428.0653	90	1	100.00	0	1.48	100.00	49.51	77.03	100.00	91.74
2787	0	180	24570.9889	15000	90	0.5	100.00	0	1.47	100.00	48.49	76.82	100.00	91.59
5024	0	90	19785.49445	19785.49445	90	0.5	100.00	0	1.47	100.00	48.51	76.37	100.00	91.56
5025	0	90	14687.64255	14687.64255	90	0.33	100.00	0	1.46	100.00	47.75	75.69	100.00	91.41
5026	0	90	11821.17389	11821.17389	90	0.25	100.00	0	1.45	100.00	47.00	75.02	100.00	91.27
2231	0	157.5	39856.13059	25000	90	1	100.00	0	1.53	100.00	44.08	75.84	100.00	90.93
2229	0	157.5	24570.9889	15000	90	0.5	100.00	0	1.52	100.00	42.98	75.19	100.00	90.74
2230	0	157.5	44856.13059	20000	90	1	100.00	0	1.57	100.00	40.04	74.90	100.00	90.33
2226	0	157.5	19375.28509	10000	90	0.33	100.00	0	1.53	100.00	40.45	74.13	100.00	90.34
1669	0	135	13642.34778	10000	90	0.25	100.00	0	1.51	100.00	40.94	73.44	100.00	90.35
1673	0	135	39856.13059	25000	90	1	100.00	0	1.57	100.00	39.65	74.33	100.00	90.24
1671	0	135	24570.9889	15000	90	0.5	100.00	0	1.57	100.00	38.44	73.72	100.00	90.04

Nr.	Longitude of Ascending Node [°]	Argument of Periapsis [°]	Apoapsis Height [km]	Periapsis Height [mkm]	Inclination [°]	OrbitPeriod / OrbitPeriod Gateway	Average Coverage Time [%]	Average Maximum Gap Duration [h]	Average Number of Assets Available [-]	Shackleton Coverage Time [%]	North Pole Coverage Time [%]	Average Far Side Coverage [%]	Maximum Far Side Coverage [%]	Score
1111	0	112.5	13642.34778	10000	90	0.25	100.00	0	1.53	100.00	39.14	72.81	100.00	90.07
553	0	90	13642.34778	10000	90	0.25	100.00	0	1.54	100.00	38.52	72.51	100.00	89.97
2225	0	157.5	29570.9889	10000	90	0.5	100.00	0	1.59	100.00	36.22	73.88	100.00	89.75
1115	0	112.5	39856.13059	25000	90	1	100.00	0	1.60	100.00	36.80	73.30	100.00	89.79
2228	0	157.5	49856.13059	15000	90	1	100.00	0	1.62	100.00	35.37	74.18	100.00	89.66
557	0	90	39856.13059	25000	90	1	100.00	0	1.61	100.00	35.77	72.81	100.00	89.62
1113	0	112.5	24570.9889	15000	90	0.5	100.00	0	1.60	100.00	35.53	72.64	100.00	89.58
548	0	90	11894.04954	8000	90	0.2	100.00	0	1.55	100.00	35.84	71.34	100.00	89.53
1668	0	135	19375.28509	10000	90	0.33	100.00	0	1.59	100.00	34.72	72.29	100.00	89.45
555	0	90	24570.9889	15000	90	0.5	100.00	0	1.60	100.00	34.54	72.12	100.00	89.41
2219	0	157.5	31570.9889	8000	90	0.5	100.00	0	1.62	100.00	32.93	73.31	100.00	89.28
1672	0	135	44856.13059	20000	90	1	100.00	0	1.64	100.00	32.77	72.49	100.00	89.20
2224	0	157.5	54856.13059	10000	90	1	100.00	0	1.67	100.00	29.44	73.40	100.00	88.82
1110	0	112.5	19375.28509	10000	90	0.33	100.00	0	1.62	100.00	31.15	70.91	100.00	88.88
1105	0	112.5	15642.34778	8000	90	0.25	100.00	0	1.61	100.00	30.65	70.36	100.00	88.78
552	0	90	19375.28509	10000	90	0.33	100.00	0	1.63	100.00	29.93	70.24	100.00	88.67
1662	0	135	21375.28509	8000	90	0.33	100.00	0	1.64	100.00	28.91	70.84	100.00	88.58
2218	0	157.5	56856.13059	8000	90	1	100.00	0	1.70	100.00	26.46	73.09	100.00	88.40
547	0	90	15642.34778	8000	90	0.25	100.00	0	1.63	100.00	29.47	69.71	100.00	88.58
1114	0	112.5	44856.13059	20000	90	1	100.00	0	1.68	100.00	28.39	70.71	100.00	88.50
1667	0	135	29570.9889	10000	90	0.5	100.00	0	1.68	100.00	27.38	70.90	100.00	88.38
556	0	90	44856.13059	20000	90	1	100.00	0	1.70	100.00	26.98	69.92	100.00	88.26
1670	0	135	49856.13059	15000	90	1	100.00	0	1.71	100.00	25.53	70.77	100.00	88.12
1104	0	112.5	21375.28509	8000	90	0.33	100.00	0	1.69	100.00	24.30	68.86	100.00	87.83
1661	0	135	31570.9889	8000	90	0.5	100.00	0	1.72	100.00	22.66	69.77	100.00	87.67
538	0	90	12219.45685	5000	90	0.17	100.00	0	1.65	100.00	24.29	67.36	100.00	87.73

Tab. 4-4 Best scores achieved after the last iteration of periapsis heights. The constellations consist of the Gateway and one additional satellite. The yellow-colored satellite achieved the highest score overall with a score of 97.6456 at a periapsis height of 10527 km.

Nr.	Longitude of Ascending Node [°]	Argument of Periapsis [°]	Apoapsis Height [km]	Periapsis Height [mkm]	Inclination [°]	OrbitPeriod / OrbitPeriod Gateway	Average Coverage Time [%]	Average Maximum Gap Duration [h]	Average Number of Assets Available [-]	Shackleton Coverage Time [%]	North Pole Coverage Time [%]	Average Far Side Coverage [%]	Maximum Far Side Coverage [%]	Score
130	0	270	54329.13059	10527	90	1	99.99999595	0	1.092226213	99.99999595	87.70566271	89.30139312	99.98551865	97.6456
131	0	270	54328.13059	10528	90	1	99.99999595	0	1.092240833	99.99999595	87.7041927	89.30077744	99.98552944	97.6453
132	0	270	54327.13059	10529	90	1	99.99999595	0	1.092255453	99.99999595	87.70272268	89.30015844	99.98554023	97.6451
133	0	270	54326.13059	10530	90	1	99.99999595	0	1.092270073	99.99999595	87.70125257	89.2995388	99.98555102	97.6449
134	0	270	54325.13059	10531	90	1	99.99999595	0	1.092284694	99.99999595	87.69978243	89.29891514	99.98556181	97.6446
135	0	270	54324.13059	10532	90	1	99.99999595	0	1.092299315	99.99999595	87.69831226	89.29828795	99.9855726	97.6444
136	0	270	54323.13059	10533	90	1	99.99999595	0	1.092313937	99.99999595	87.69684206	89.29765658	99.98558339	97.6442
137	0	270	54322.13059	10534	90	1	99.99999595	0	1.092328559	99.99999595	87.69537176	89.29702015	99.98559418	97.6439
138	0	270	54321.13059	10535	90	1	99.99999595	0	1.092343182	99.99999595	87.69390147	89.29637746	99.98560498	97.6437
139	0	270	54320.13059	10536	90	1	99.99999595	0	1.092357805	99.99999595	87.69243115	89.29572663	99.98561577	97.6435
140	0	270	54319.13059	10537	90	1	99.99999595	0	1.092372429	99.99999595	87.69096078	89.29506451	99.98562656	97.6432
141	0	270	54318.13059	10538	90	1	99.99999595	0	1.092387053	99.99999595	87.68949037	89.29438595	99.98563736	97.643
142	0	270	54317.13059	10539	90	1	99.99999595	0	1.092401678	99.99999595	87.68801991	89.29367925	99.98564815	97.6427
143	0	270	54316.13059	10540	90	1	99.99999595	0	1.092416303	99.99999595	87.6865494	89.29290254	99.98565895	97.6425
144	0	270	54315.13059	10541	90	1	99.99999595	0	1.092430928	99.99999595	87.68507882	89.29206592	99.98566974	97.6422
145	0	270	54314.13059	10542	90	1	99.99999595	0	1.092445554	99.99999595	87.68360819	89.29150742	99.98568054	97.642
146	0	270	54313.13059	10543	90	1	99.99999595	0	1.092460181	99.99999595	87.68213759	89.29094892	99.98569133	97.6418
147	0	270	54312.13059	10544	90	1	99.99999595	0	1.092474808	99.99999595	87.68066694	89.29039042	99.98570213	97.6415
148	0	270	54311.13059	10545	90	1	99.99999595	0	1.092489435	99.99999595	87.67919621	89.28983195	99.98571292	97.6413
149	0	270	54310.13059	10546	90	1	99.99999595	0	1.092504063	99.99999595	87.67772545	89.28927346	99.98572372	97.6411
150	0	270	54309.13059	10547	90	1	99.99999595	0	1.092518691	99.99999595	87.67625465	89.28871502	99.98573452	97.6408
151	0	270	54308.13059	10548	90	1	99.99999595	0	1.09253332	99.99999595	87.6747838	89.28815658	99.98574532	97.6406
152	0	270	54307.13059	10549	90	1	99.99999595	0	1.092547949	99.99999595	87.67331292	89.28759813	99.98575612	97.6404
153	0	270	54306.13059	10550	90	1	99.99999595	0	1.092562579	99.99999595	87.67184197	89.2870397	99.98576692	97.6401
154	0	270	54305.13059	10551	90	1	99.99999595	0	1.092577209	99.99999595	87.670371	89.28648128	99.98577772	97.6399
155	0	270	54304.13059	10552	90	1	99.99999595	0	1.09259184	99.99999595	87.6689	89.28592287	99.98578852	97.6397
156	0	270	54303.13059	10553	90	1	99.99999595	0	1.092606471	99.99999595	87.66742896	89.28536448	99.98579932	97.6395
157	0	270	54302.13059	10554	90	1	99.99999595	0	1.092621103	99.99999595	87.66595784	89.2848061	99.98581012	97.6392
158	0	270	54301.13059	10555	90	1	99.99999595	0	1.092635735	99.99999595	87.66448673	89.28424772	99.98582092	97.639
159	0	270	54300.13059	10556	90	1	99.99999595	0	1.092650368	99.99999595	87.66301557	89.28368936	99.98583172	97.6388
160	0	270	54299.13059	10557	90	1	99.99999595	0	1.092665001	99.99999595	87.66154435	89.283131	99.98584252	97.6385
161	0	270	54298.13059	10558	90	1	99.99999595	0	1.092679634	99.99999595	87.66007309	89.28257265	99.98585333	97.6383
162	0	270	54297.13059	10559	90	1	99.99999595	0	1.092694268	99.99999595	87.65860176	89.2820143	99.98586413	97.6381
163	0	270	54296.13059	10560	90	1	99.99999595	0	1.092708902	99.99999595	87.65713037	89.28145598	99.98587493	97.6378
164	0	270	54295.13059	10561	90	1	99.99999595	0	1.092723537	99.99999595	87.65565897	89.28089766	99.98588574	97.6376
165	0	270	54294.13059	10562	90	1	99.99999595	0	1.092738173	99.99999595	87.65418758	89.28033935	99.98589654	97.6374
166	0	270	54293.13059	10563	90	1	99.99999595	0	1.092752808	99.99999595	87.65271612	89.27978105	99.98590733	97.6371
167	0	270	54292.13059	10564	90	1	99.99999595	0	1.092767445	99.99999595	87.6512446	89.27922276	99.98591814	97.6369
168	0	270	54291.13059	10565	90	1	99.99999595	0	1.092782081	99.99999595	87.64977304	89.27866449	99.98592895	97.6367
169	0	270	54290.13059	10566	90	1	99.99999595	0	1.092796718	99.99999595	87.64830138	89.27810622	99.98593975	97.6364

Nr.	Longitude of Ascending Node [°]	Argument of Periapsis [°]	Apoapsis Height [km]	Periapsis Height [mkm]	Inclination [°]	OrbitPeriod / OrbitPeriod Gateway	Average Coverage Time [%]	Average Maximum Gap Duration [h]	Average Number of Assets Available [-]	Shackleton Coverage Time [%]	North Pole Coverage Time [%]	Average Far Side Coverage [%]	Maximum Far Side Coverage [%]	Score
170	0	270	54289.13059	**10567**	90	1	99.99999595	0	1.092811356	99.99999595	87.64682973	89.27754797	99.98595056	97.6362
171	0	270	54288.13059	**10568**	90	1	99.99999595	0	1.092825994	99.99999595	87.64535803	89.27698972	99.98596137	97.636
172	0	270	54287.13059	**10569**	90	1	99.99999595	0	1.092840633	99.99999595	87.64388625	89.2764315	99.98597218	97.6357
173	0	270	54286.13059	**10570**	90	1	99.99999595	0	1.092855272	99.99999595	87.6424145	89.27587328	99.98598298	97.6355
174	0	270	54285.13059	**10571**	90	1	99.99999595	0	1.092869912	99.99999595	87.64094268	89.27531506	99.98599379	97.6353
175	0	270	54284.13059	**10572**	90	1	99.99999595	0	1.092884552	99.99999595	87.63947081	89.27475685	99.9860046	97.635
176	0	270	54283.13059	**10573**	90	1	99.99999595	0	1.092899192	99.99999595	87.63799891	89.27419865	99.98601541	97.6348
177	0	270	54282.13059	**10574**	90	1	99.99999595	0	1.092913833	99.99999595	87.63652698	89.27364045	99.98602622	97.6346
178	0	270	54281.13059	**10575**	90	1	99.99999595	0	1.092928475	99.99999595	87.63505497	89.27308228	99.98603703	97.6344
179	0	270	54280.13059	**10576**	90	1	99.99999595	0	1.092943116	99.99999595	87.63358293	89.27252411	99.98604784	97.6341
180	0	270	54279.13059	**10577**	90	1	99.99999595	0	1.092957759	99.99999595	87.63211088	89.27196595	99.98605866	97.6339
181	0	270	54278.13059	**10578**	90	1	99.99999595	0	1.092972401	99.99999595	87.63063873	89.27140781	99.98606947	97.6337
182	0	270	54277.13059	**10579**	90	1	99.99999595	0	1.092987045	99.99999595	87.62916657	89.27084966	99.98608028	97.6334
183	0	270	54276.13059	**10580**	90	1	99.99999595	0	1.093001688	99.99999595	87.62769436	89.27029154	99.98609109	97.6332
184	0	270	54275.13059	**10581**	90	1	99.99999595	0	1.093016333	99.99999595	87.62622213	89.26973342	99.98610191	97.633
185	0	270	54274.13059	**10582**	90	1	99.99999595	0	1.093030977	99.99999595	87.62474984	89.26917532	99.98611272	97.6327
186	0	270	54273.13059	**10583**	90	1	99.99999595	0	1.093045623	99.99999595	87.62327752	89.26861722	99.98612354	97.6325
187	0	270	54272.13059	**10584**	90	1	99.99999595	0	1.093060268	99.99999595	87.62180516	89.26805914	99.98613435	97.6323
188	0	270	54271.13059	**10585**	90	1	99.99999595	0	1.093074914	99.99999595	87.62033273	89.26750106	99.98614517	97.632
189	0	270	54270.13059	**10586**	90	1	99.99999595	0	1.093089561	99.99999595	87.61886024	89.26694299	99.98615598	97.6318
190	0	270	54269.13059	**10587**	90	1	99.99999595	0	1.093104208	99.99999595	87.61738773	89.26638493	99.9861668	97.6316
191	0	270	54268.13059	**10588**	90	1	99.99999595	0	1.093118855	99.99999595	87.61591523	89.26582689	99.98617762	97.6313
—	—	—	—	—	—	—	—	—	—	—	—	—	—	—
203	0	270	54256.13059	**10600**	90	1	99.99999595	0	1.093294661	99.99999595	87.59824152	89.25913115	99.98630746	97.6285
9	0	270	54156.13059	**10700**	90	1	99.99999595	0	1.094762312	99.99999595	87.45072393	89.2033873	99.98739202	97.6053
7	0	270	54356.13059	**10500**	90	1	99.99994968	14.68128166	1.091831665	99.99999595	87.7453364	89.3166125	99.98522751	96.5643